Memo: Library VTD for computation of VLBI time delay. Description of the algorithm.

L. Petrov
Leonid.Petrov@lpetrov.net

Revision of 2014.08.21

An algorithm for computing VLBI time delay partial derivatives with respect to parameters of the model, the algorithm of parameter estimation is described.

1 Introduction

The method of VLBI first proposed by [Matveenko et al.(1965)] allows to measure precisely the time delay and its rate of change. The time delay is defined as *a difference between two intervals: a) the interval of proper time measured by clocks of the first station between events: arrival the wavefront to the reference point of the first antenna and clock synchronization and b) the interval of proper time measured by clocks of the second station between events: arrival the wavefront to the reference point of the second antenna and clock synchronization.* The post-correlator software evaluates the time delay and its time derivative to a certain moment of time at time scale TAI called *fringe reference time* within the interval of observation, which is typically 20–700 second long.

In this paper, the algorithm for computing the time delay and delay rate is presented in chapter 2. The order of narration in this chapter follows the order of derivation of this quantity: first the expression for the time delay will be derived, then the algorithm for computing of position of the emitter and receivers in the inertial coordinate system, is described. The motion of receivers is decomposed into rotation and deformation. Then effects of propagation in refractive medium are taken into account. Finally, the coupling effects are taken into account.

The chapter 3 follows the order of computing the intermediate quantities which will be finally substituted in the expression for time delay and delay rate. Description of formats of input files needed for implementation of calculation is presented in document `vtd_format.txt` .

The truncation level for computation is 10^{-13} s for delay and 10^{-16} s/s for delay rate. If the apriori were perfect the accuracy for time delay computation would be at that level. In practice, the theoretical path delay can be predicted with the error of $1\text{–}10 \cdot 10^{-9}$ s.

2 Algorithm for computation of the theoretical path delay, delay rate and partial derivatives with respect to parameters of model

2.1 Expression for geometric path delay

Let us have two stations #1 and #2. Reference station #1 receives a radio wave form source a in time t_1 according to its local clock which are assumed synchronized with TAI via GPS. Remote station #2 receives a radio wave from the emitter e in time t_2 according to its clock which are also assumed synchronized with TAI via GPS. The problem is, knowing position and velocity of stations #1, #2, and object a, what will be the time t_2?

We have three events: emission of the radio wave with coordinates $\vec{\mathbf{R}}_e, T_e$ in a barycentric coordinate system and two events of receiving that radio wave at stations #1 and #2 with coordinates $\vec{\mathbf{r}}_1, t_1$, $\vec{\mathbf{r}}_2, t_2$ in a geocentric coordinate system.

The post Newtonian metric in these coordinates can be written this way:

$$\begin{aligned} G_{00} &= 1 - 2\frac{U}{c^2} + 2Ł_b + O(1/c^4) \\ G_{0k} &= O(1/c^3) \\ G_{mn} &= -\delta_{mn}\left(1 + 2\frac{U}{c^2} - 2Ł_b\right) + O(1/c^4) \end{aligned} \tag{1}$$

$$\begin{aligned} g_{00} &= 1 - 2\frac{U_\oplus}{c^2} + 2Ł_g + O(1/c^4) \\ g_{0k} &= O(1/c^3) \\ g_{mn} &= -\delta_{mn}\left(1 + 2\frac{U_\oplus}{c^2} - 2Ł_g\right) + O(1/c^4) \end{aligned} \tag{2}$$

for the barycentric and geocentric coordinate systems respectively. Here U is the sum of the gravitational potential of all external bodies in the geocenter, $U_\oplus$ — geopotential, L_b and L_g are some arbitrary scaling constants. Their numerical values depends on a convention. Parameters L_b and L_g were introduced into the expression for the metric artificially. Equations of general relativity allows scaling transformation. When the coordinate system is defined, 7 parameters should be specified: three parameters of the origin, three parameters of orientation, and *the scaling parameter*. In physics usually $L_b = L_g = 0$. That implies that in the infinity the metric tensor becomes the Minkowsky tensor. In geodesy various values for L_b and L_g were used:

- TDB baricenteric coordinate system, $L_b = \frac{fM_\odot}{\bar{R}_\odot c^2} = 1.48082686741 \cdot 10^{-8}$, $L_g = 0$;
- ITRF2000 (or IERS1992) geocentric coordinate system, $L_b = 0$; $L_g = 6.969290134 \cdot 10^{-10} \approx \frac{fM_\oplus}{\bar{R}_\oplus c^2} + \frac{2}{3c^2}\Omega_\oplus^2 R_\oplus$;
- IAU2000 baricenteric coordinate system, $L_b = L_g = 0$.
- IERS1996 geocentric coordinate system, $L_b = 0$; $L_g = -\frac{fM_\oplus}{\bar{R}_\oplus c^2} = -6.969290134 \cdot 10^{-10} \approx -\frac{fM_\oplus}{\bar{R}_\oplus c^2} - \frac{2}{3c^2}\Omega_\oplus^2 R_\oplus$;

where $\Omega_\oplus$ is the nominal Earth's angular velocity.

Since coordinates of the emitter are represented in the barycentric coordinate system, let us first compute time delay as the difference of barycentric time coordinates and then transform it to the difference of intervals of proper time which are related to quantities derived from analysis of VLBI fringe phases.

First, transform coordinates $\vec{\mathbf{r}}_1, t_1$, $\vec{\mathbf{r}}_2, t_2$ from the geocentric to the barycentric coordinate system. Using expression for metric (1), (2) we find

$$\begin{aligned}
\vec{\mathbf{R}}_1(T_1) &= \left(1 - \left(\frac{U_\odot}{c^2} - L_b\right)\right)\vec{\mathbf{r}}_1 - \frac{1}{2c^2}\left(\vec{\mathbf{V}}_\oplus \vec{\mathbf{R}}_\oplus\right)\vec{\mathbf{V}}_\oplus \\
\vec{\mathbf{R}}_2(T_1) &= \left(1 - \left(\frac{U_\odot}{c^2} - L_b\right)\right)\vec{\mathbf{r}}_2 - \frac{1}{2c^2}\left(\vec{\mathbf{V}}_\oplus \vec{\mathbf{R}}_\oplus\right)\vec{\mathbf{V}}_\oplus \\
T_1 &= t_1 + \frac{1}{c^2}\,\vec{\mathbf{r}}_1\,\vec{\mathbf{V}}_\oplus + \frac{1}{c^2}\int\limits_{t_0}^{t}\left(\frac{1}{2}v^2 + U\right)dt + 32.184
\end{aligned} \tag{3}$$

Here we retain only contribution of the gravitational potential of the Sun.

The barycentric travel time of the signal from the emitter a to station #1 and to station #2 are

$$\begin{aligned}
T_1 - T_e = {} & \frac{1}{c}\left|\vec{\mathbf{R}}_e(T_e) - \vec{\mathbf{R}}_1(T_1)\right| + T_{1,grav} \\
T_2 - T_e = {} & \frac{1}{c}\left|\vec{\mathbf{R}}_e(T_e) - \vec{\mathbf{R}}_2(T_2)\right| + T_{2,grav} \\
T_{i,grav} = {} & \sum_k \frac{2fM_k}{c^3} \\
& \left(1 + \frac{1}{c}\dot{\vec{\mathbf{R}}}_k(T'_e)\underline{\vec{\mathbf{S}}}(T_i, T'_e)\right)\ln\left(|\vec{\mathbf{R}}_e(T_e) - \vec{\mathbf{R}}_k(T'_e)| + (\vec{\mathbf{R}}_e(T_e) - \vec{\mathbf{R}}_k(T'_e))\underline{\vec{\mathbf{S}}}(T_i, T'_e)\right) - \\
& \left(1 + \frac{1}{c}\dot{\vec{\mathbf{R}}}_k(T'_k)\underline{\vec{\mathbf{S}}}(T_i, T'_e)\right)\ln\left(|\vec{\mathbf{R}}_i(T_i) - \vec{\mathbf{R}}_k(T'_e)| + (\vec{\mathbf{R}}_i(T_i) - \vec{\mathbf{R}}_k(T'_e))\underline{\vec{\mathbf{S}}}(T_i, T'_e)\right)
\end{aligned} \tag{4}$$

where f is the universal gravitational constant, M_k is the mass of the gravitating body, summation is done over all big planets of the Solar system, excluding the Pluto, but including the Moon. Position of the gravitating body in (4) is taken in the retarded moment of barycentric time T'_k which is a solution of the gravitation null-cone equation:

$$T'_k = T_1 - \frac{1}{c}\left|\vec{\mathbf{R}}_1(T_1) - \vec{\mathbf{R}}_k(T'_k)\right| \tag{5}$$

Retarded moment of emission T'_e is a solution of a similar gravitation null-cone equation:

$$T'_e = T_1 - \frac{1}{c}\left|\vec{\mathbf{R}}_1(T_1) - \vec{\mathbf{R}}_k(T'_e)\right| \tag{6}$$

The vector towards the source $\underline{\vec{\mathbf{S}}}(T_i, T_e)$ is

$$\underline{\vec{\mathbf{S}}}(T_i, T'_e) = \frac{\vec{\mathbf{R}}_i(T_i) - \vec{\mathbf{R}}_e(T'_e)}{|\vec{\mathbf{R}}_i(T_i) - \vec{\mathbf{R}}_e(T'_e)|} \tag{7}$$

Derivation of expression (4) was made by many authors. At present, one of the most comprehensive papers is the article of [Kopeikin and Shaeffer, 1999]. For solving equations (4) two cases should be considered separately, when the object is in the far zone, i.e. we can consider the wavefront flat, and the case one cannot neglect wavelength curvature. This happens when the diurnal parallax of the object exceeds the error of delay computation, $\sigma\tau/|\tau|, 10^{-11}$ in our case. This is true for the objects within the Solar System.

2.1.1 VLBI time delay for a far zone object

In the case, when $\dfrac{|R_i|}{|R_e|} < \sigma_\tau/|\tau|$ expression for gravitational excess delay (4) $\tau_{grav} = T_{1,grav} - T_{2,grav}$ is reduced to

$$\tau_{grav} = 2\sum_{k=1}\frac{f\,M_k}{c^3}\left(1+\frac{1}{c}\dot{\vec{\mathbf{R}}}_k(T'_{1k})\cdot\underline{\vec{\mathbf{S}}}\right)\ln\frac{|\vec{\mathbf{R}}_k(T'_k)-\vec{\mathbf{R}}_1|+\underline{\vec{\mathbf{S}}}\cdot(\vec{\mathbf{R}}_k(T'_k)-\vec{\mathbf{R}}_1)}{|\vec{\mathbf{R}}_k(T'_k)-\vec{\mathbf{R}}_2|+\underline{\vec{\mathbf{S}}}\cdot(\vec{\mathbf{R}}_k(T'_k)-\vec{\mathbf{R}}_2)} \tag{8}$$

Implicit equation for time delay (4) can be simplified using by expanding it in series. For any vector $\vec{\mathbf{A}}$ and $\vec{\mathbf{b}}$ such that $|\vec{\mathbf{b}}| \ll |\vec{\mathbf{A}}|$ the module of their difference $|\vec{\mathbf{A}}-\vec{\mathbf{b}}|$ can be expressed as

$$|\vec{\mathbf{A}}-\vec{\mathbf{b}}| = |A| + \vec{\mathbf{a}}\cdot\vec{\mathbf{b}} + O\left(\frac{b^2}{|A|}\right) \tag{9}$$

where $\vec{\mathbf{a}} = \dfrac{A}{|A|}$. Then the difference of barycentric time coordinates can be written as

$$T_2 - T_1 = \frac{1}{c}\left(\vec{\mathbf{R}}_1(T_1)-\vec{\mathbf{R}}_2(T_2)\right)\underline{\vec{\mathbf{S}}} + \tau_{grav} + \tau_p \tag{10}$$

where τ_p is an additional delay which takes into account extra delay caused by the propagation media.

After expansion $\vec{\mathbf{R}}_2(T_2)$ near instant T_2 as

$$\vec{\mathbf{R}}_2(T_2) = \vec{\mathbf{R}}_2(T_1) + \dot{\vec{\mathbf{R}}}_2(T_1)(T_2-T_1) + O(\ddot{\vec{\mathbf{R}}}_2(T_2-T_1)^2) \tag{11}$$

we have

$$T_2 - T_1 = \frac{1}{c}\frac{\left(R_1(T_1)-R_2(T_2)\right)\cdot\underline{\vec{\mathbf{S}}} + \tau_{grav} + \tau_p}{1+\dfrac{1}{c}\dot{\vec{\mathbf{R}}}_2(T_1)\cdot\underline{\vec{\mathbf{S}}}} \tag{12}$$

Now we should relate baricenteric vectors of site positions with geocentric vector coordinate and transform the difference of baricenteric time coordinates $T_2 - T_1$ to the difference of intervals of proper time between events of coming the wavefront to stations #1 and #2 and clock syncrhonization. The differences of barycentric time coordinates $T_1 - T_{sync}$ and $T_2 - T_{sync}$ are first to transformed to geocentric coordinate system, then these differences of geocentric time coordinates are transformed to intervals of proper time.

Term $\dfrac{1}{c^2}\int\left(\dfrac{1}{2}v^2 + U\right)dt$ in 3 deserves special consideration. This sum of centrifugal and gravitational potential describes the difference in clock rate at a station with respect to the geocentric time. First, notice, time as measured by station clock synchronized in TAI or TT[1]. TAI cooresponds to proper time of a hypotetical clock on the geoid. For a sta-

[1]TT - TAI = 32.184

tion that has the height above the geoid, so-called orthometric height, this term is reduced $-\frac{1}{c^2}\int\left(\frac{2}{3}\Omega_\oplus^2 R_\oplus \cos^2\varphi \,+\, g_{loc}\right)h_{ort}\,dt$, where g_{loc} is the local gravity acceleration. Neglecting site position variations due to tides and mass loading, the expression under integral is constant. Integration will give a linear trend and an arbitrary integration constant. The value of the constant corresponds to clock syncrhonization that occurs before the experiment start.

Finally, we get the following expression for time delay in the far zone:

$$\begin{aligned}
&\Big((t_{2p}-t_{sync})-(t_{1p}-t_{sync})\Big)(t_1) = \\
&\frac{1}{1+\frac{1}{c}(\vec{\mathbf{V}}_\oplus+\dot{\vec{\mathbf{r}}}_2)\cdot\underline{\vec{\mathbf{S}}}}\left(\frac{1}{c}(\vec{\mathbf{r}}_1(t_1)-\vec{\mathbf{r}}_2(t_1))\cdot\underline{\vec{\mathbf{S}}}\left[1-\left(2\frac{fM_\odot}{|\vec{\mathbf{R}}_\oplus|c^2}-L_b\right)-\left(\frac{U_\oplus}{c^2}-L_g\right)-\frac{|\vec{\mathbf{V}}_\oplus|^2}{2c^2}-\right.\right. \\
&\left.\left.\frac{\vec{\mathbf{V}}_\oplus\cdot\dot{\vec{\mathbf{r}}}_2}{c^2}\right]+\frac{1}{c^2}\vec{\mathbf{V}}_\oplus\cdot(\vec{\mathbf{r}}_1(t_1)-\vec{\mathbf{r}}_2(t_1))\left(1+\frac{1}{2c}\vec{\mathbf{V}}_\oplus\cdot\underline{\vec{\mathbf{S}}}\right)-\frac{1}{c}\,\rho\,(\vec{\mathbf{r}}_1(t_1)-\vec{\mathbf{r}}_2(t_1))\,\frac{\vec{\mathbf{R}}_\oplus}{\bar{D}_\oplus}+\tau_{grav}+\tau_p\right)- \\
&\frac{1}{c^2}\left(g_{loc,2}\,h_{ort,2}-g_{loc,1}\,h_{ort,1}+\frac{2}{3}R_\oplus\Omega_\oplus^2\,(\cos^2\varphi_{gc,2}\,h_{ort,2}-\cos^2\varphi_{gc,1}\,h_{ort,1})\right)\cdot(t_{1p}-t_{sync})
\end{aligned} \tag{13}$$

where ρ is the annual parallax of the observed source, φ is geocentric latitude, and $\bar{D}_\oplus$ is the mean distance between the barycenter of the Solar System and the barycenter the system Earth–Moon (astronomical unit). We can neglect dependence of the gravitational potential on height for ground stations and compute it as $U_\oplus = \dfrac{fM_\oplus}{|r_\oplus|}$ and omite v_2^2/c^2 for ground stations.

The time delay is itself a function of time. The argument of its time dependence is the geocentric time t_1 of the event of wavefront coming to reference station #1. Differentiating this expression with respect to time and discarding terms which are less than 10^{-16}, we get

$$\begin{aligned}
&\frac{\partial}{\partial t}\Big((t_{2p}-t_{sync})-(t_{1p}-t_{sync})\Big)(t_1) = \\
&\frac{1}{1+\frac{1}{c}(\vec{\mathbf{V}}_\oplus+\dot{\vec{\mathbf{r}}}_2)\cdot\underline{\vec{\mathbf{S}}}}\left(\frac{1}{c}(\dot{\vec{\mathbf{r}}}_1-\dot{\vec{\mathbf{r}}}_2)\cdot\underline{\vec{\mathbf{S}}}\left[1-\left(2\frac{fM_\odot}{|\vec{\mathbf{R}}_\oplus|c^2}-L_b\right)-\left(\frac{U_\oplus}{c^2}-L_g\right)-\frac{|\vec{\mathbf{V}}_\oplus|^2}{2c^2}-\frac{\vec{\mathbf{V}}_\oplus\cdot\dot{\vec{\mathbf{r}}}_2}{c^2}\right]+\right. \\
&\frac{1}{c^2}\left(\dot{\vec{\mathbf{V}}}_\oplus\cdot(\vec{\mathbf{r}}_1-\vec{\mathbf{r}}_2)+\vec{\mathbf{V}}_\oplus\cdot(\dot{\vec{\mathbf{r}}}_1-\dot{\vec{\mathbf{r}}}_2)\right)\left(1+\frac{1}{2c}\vec{\mathbf{V}}_\oplus\cdot\underline{\vec{\mathbf{S}}}\right)-\frac{1}{c}\,\rho\,(\dot{\vec{\mathbf{r}}}_1-\dot{\vec{\mathbf{r}}}_2)\,\frac{\vec{\mathbf{R}}_\oplus}{\bar{D}_\oplus}+\tfrac{\partial}{\partial t}\tau_{grav}+\tfrac{\partial}{\partial t}\tau_p\Big)- \\
&\frac{1}{c}\frac{(\dot{\vec{\mathbf{V}}}_\oplus+\ddot{\vec{\mathbf{r}}}_2)\cdot\underline{\vec{\mathbf{S}}}}{\left(1+\frac{1}{c}(\vec{\mathbf{V}}_\oplus+\dot{\vec{\mathbf{r}}}_2)\cdot\underline{\vec{\mathbf{S}}}\right)^2}\left(\frac{1}{c}(\vec{\mathbf{r}}_1-\vec{\mathbf{r}}_2)\cdot\underline{\vec{\mathbf{S}}}+\frac{1}{c^2}\vec{\mathbf{V}}_\oplus\cdot(\vec{\mathbf{r}}_1-\vec{\mathbf{r}}_2)+\frac{1}{c}\,\rho\,(\vec{\mathbf{r}}_1-\vec{\mathbf{r}}_2)\,\frac{\vec{\mathbf{R}}_\oplus}{\bar{D}_\oplus}+\tau_{grav}+\tau_p\right)- \\
&\frac{1}{c^2}\left(g_{loc,2}\,h_{ort,2}-g_{loc,1}\,h_{ort,1}+\frac{2}{3}R_\oplus\Omega_\oplus^2\,(\cos^2\varphi_2\,h_{ort,2}-\cos^2\varphi_1\,h_{ort,1})\right)
\end{aligned} \tag{14}$$

and

$$\begin{aligned}\frac{\partial}{\partial t}\tau_{grav} &= 2\sum_{k=1}\frac{f\,M_k}{c^3}\left(1+\underline{\vec{S}}\cdot\ddot{\vec{\mathbf{R}}}_k(T'_{1k})\right)\ln\frac{|\vec{\mathbf{R}}_k(T'_k)-\vec{\mathbf{R}}_1|+\underline{\vec{S}}\cdot(\vec{\mathbf{R}}_k(T'_k)-\vec{\mathbf{R}}_1)}{|\vec{\mathbf{R}}_k(T'_k)-\vec{\mathbf{R}}_2|+\underline{\vec{S}}\cdot(\vec{\mathbf{R}}_k(T'_k)-\vec{\mathbf{R}}_2)}+\\ &2\sum_{k=1}\frac{f\,M_k}{c^3}\left(1+\underline{\vec{S}}\cdot\dot{\vec{\mathbf{R}}}_k(T'_{1k})\right)\cdot\\ &\left(\frac{-\dfrac{\dot{\vec{\mathbf{R}}}_k(T'_k)\cdot\vec{\mathbf{R}}_1+\vec{\mathbf{R}}_k(T'_k)\cdot\dot{\vec{\mathbf{R}}}_1}{|\vec{\mathbf{R}}_k(T'_k)-\vec{\mathbf{R}}_1|}+(\dot{\vec{\mathbf{R}}}_k(T'_k)-\dot{\vec{\mathbf{R}}}_1)\cdot\vec{S}}{|\vec{\mathbf{R}}_k(T'_k)-\vec{\mathbf{R}}_1|+(\vec{\mathbf{R}}_k(T'_k)-\vec{\mathbf{R}}_1)\cdot\vec{S}}-\right.\\ &\left.\frac{-\dfrac{\dot{\vec{\mathbf{R}}}_k(T'_k)\cdot\vec{\mathbf{R}}_2+\vec{\mathbf{R}}_k(T'_k)\cdot\dot{\vec{\mathbf{R}}}_2}{|\vec{\mathbf{R}}_k(T'_k)-\vec{\mathbf{R}}_2|}+(\dot{\vec{\mathbf{R}}}_k(T'_k)-\dot{\vec{\mathbf{R}}}_2)\cdot\vec{S}}{|\vec{\mathbf{R}}_k(T'_k)-\vec{\mathbf{R}}_2|+(\vec{\mathbf{R}}_k(T'_k)-\vec{\mathbf{R}}_2)\cdot\vec{S}}\right)\end{aligned}\tag{15}$$

In practice, the last term, linear in time for time delay and constant for delay rate is usually ignored since it is not distingioshable from the Hydrogen clock frequency offset. This term is solved for during post-processing dat aanalysis.

2.1.2 VLBI time delay when one of antenna is at the Earth's orbit

One of the elements of the radiointerferometer may be at the Earth's orbit. Equations for time delay and its time derivatives 13–15 remain valid for this case, except the last term that accounts for difference in clock rate. The satellite orbit should be transformed to the geocentric coordinate system with the same expression for metric as for coordinates of ground stations before computations.

In the case if the orbiting station has the clock that preserves its count through the entire experiment, the path delay is computed the same way as for the baseline between ground stations, except the fact that the ground and the orbiting station have different model of their motion.

The orbiting station may or may not have a continuous time counter. For instance, Radioastron has its on-board Hydrogen maser clock that feeds both the receiver and the sampler, but the sample counter is implicitly reset at the beginning of each scan (Y. Kovalev (2012), private communication). The reading of the clock of the ground downlink station is written in the time tag field in the scan header of data record of the orbiting telescope. It should be stressed that the delay is still determined as a difference of intervals proper time between events of coming the wavefront to the station and clock synchronization measured with station clocks for both ground station and orbiting station. It is the on-board clock that generates the rail of samples and send the digitized samples down to the Earth. The interval of time of each sample relative to the first sample of a scan is the proper time of the on-board clock.

Clock synchronization usually done only once per experiment for ground stations. For the orbiting station without a continuous time counter, clock synchronization is done at the beginning of each scan. The difference between the time coordinate at the orbiting station t_s and the time coordinate at the downlink station t_d for the observer at the downlink station can be found by solving the light-cone equation

$$t_s - t_d = \frac{1}{c}|\vec{\mathbf{r}}_s(t_d+(t_s-t_d)) - \vec{\mathbf{r}}_d| \tag{16}$$

where $\vec{\mathbf{r}}_d$ is the position of the downlink station in the geocentric coordinate system and $\vec{\mathbf{r}}_s$ is the position of the satellite in the geocentric coordinate system according to its ephemeride.

This equation is solved by iterations. Then the time tag of the first sample of a scan from the orbiting telescope is $t_d - (t_s - t_d)$. For ground station the a priori clock model is computed from results of clock synchronization before and after experiment. The difference between the sampler clock minus TAI is approximated with a liner function and subtracted from the geometric path delay. For the orbiting station without a continuous time counter, clock of the downlink station is synchronized against TAI using the same way as for other ground stations. Then the delay between the orbiting and the downlink station, $t_s - t_d$, considered constant for each scan, is added to the geometric delay. This difference represents the clock synchronization errors and is constant for every sample of a scan. For the next scan a new difference $t_s - t_d$ is computed for the time of recording the first sample.

In the case if the second station of a baseline is on the orbit, $\tau\,\vec{v}_2^2/c^2$ is not negligible and $U_\oplus$ cannot be computed as $\dfrac{fM_\oplus}{R_\oplus}$ in expression 13–14. We need to add the following terms τ_a and $\dfrac{\partial}{\partial t}\tau_a$ to expressions 13–14:

$$\begin{aligned}
\tau_a &= -\frac{\vec{v}_2^2}{2c^2}(\vec{\mathbf{r}}_1 - \vec{\mathbf{r}}_2)\cdot\vec{\underline{\mathbf{S}}} + \frac{fM_\oplus}{c^2}\left(\tfrac{1}{|\vec{\mathbf{r}}_2|} - \tfrac{1}{R_\oplus}\right)\vec{\mathbf{r}}_2\cdot\vec{\underline{\mathbf{S}}} \\
\frac{\partial}{\partial t}\tau_a &= -\frac{\vec{v}_2^2}{2c^2}(\dot{\vec{\mathbf{r}}}_1 - \dot{\vec{\mathbf{r}}}_2)\cdot\vec{\underline{\mathbf{S}}} + \frac{fM_\oplus}{c^2}\left(\tfrac{1}{|\vec{\mathbf{r}}_2|} - \tfrac{1}{R_\oplus}\right)\dot{\vec{\mathbf{r}}}_2\cdot\vec{\underline{\mathbf{S}}}
\end{aligned} \tag{17}$$

In the case if the first station of a baseline is on the orbit, corrections τ_b and $\dfrac{\partial}{\partial t}\tau_b$ should be added to expressions 13–14:

$$\begin{aligned}
\tau_b &= -\frac{fM_\oplus}{c^2}\left(\tfrac{1}{|\vec{\mathbf{r}}_1|} - \tfrac{1}{R_\oplus}\right)\vec{\mathbf{r}}_1\cdot\vec{\underline{\mathbf{S}}} \\
\frac{\partial}{\partial t}\tau_b &= -\frac{fM_\oplus}{c^2}\left(\tfrac{1}{|\vec{\mathbf{r}}_1|} - \tfrac{1}{R_\oplus}\right)\dot{\vec{\mathbf{r}}}_1\cdot\vec{\underline{\mathbf{S}}}
\end{aligned} \tag{18}$$

In a case of a ground station term $\dfrac{1}{c^2}\int\left(\dfrac{1}{2}v^2 + U\right)dt$ is reduced to a small linear function with rate approximately $10^{-16}\cdot h_{ort}$. Since velocity and distance to the spacecraft is changing during experiment, this term cannot be reduced. Instead, we have to integrate this expression

$$\Delta t = \frac{1}{c^2}\int\limits_{t_{s,sync}}^{t_{s,obs}}\left(\frac{1}{2}\dot{r}_s^2(t) + \frac{fM_\oplus}{|r_s(t)|} - \frac{fM_\oplus}{R_\oplus} - \frac{2}{3}\Omega_\oplus^2 R_\oplus^2 + fM_{moon}\left(\frac{1}{|r_s(t)|} - \frac{1}{|R_\oplus|}\right)\right)dt \tag{19}$$

using satellite ephemerides. I emphasize here in the lower and upper limits that the time coordinate at the orbiting satellite should be used that is related to downlink station time t_d via expression 16.

For observations with the orbiting station that does not have a sample counter, clock synchronization occurs at the nominal start time. Term Δt is either added if the orbiting station is a reference station #1 or subtracted if the orbiting station is a remote station #2.

2.1.3 VLBI time delay for a near zone object

If the object is in the near zone, then the most straightforward way of solving equations (4) is the method of consecutive iterations. At the first iteration we set the the right-hand side $T_{ap} := T_1, \quad T_k'^p := T_1$ and $T_{2p} := T_2$. Then

$$
\begin{aligned}
T_e \quad &:= T_{ap} \; - \; \frac{1}{c}\left|\vec{\mathbf{R}}_e(T_{ap}) - \vec{\mathbf{R}}_1(T_1)\right| \; - \; T^p_{grav_1} \\
T'_k \quad &:= T_1 - \frac{1}{c}\left|\vec{\mathbf{R}}_1(T_1) - \vec{\mathbf{R}}_k(T_k'^p)\right| \\
T^p_{grav_1} \quad &= \sum_k \frac{2fM_k}{c^3}\log\left|\frac{|\vec{\mathbf{R}}_k(T_k'^p) - \vec{\mathbf{R}}_e(T_{ap})| \; + \; |\vec{\mathbf{R}}_k(T_k'^p) - \vec{\mathbf{R}}_1(T_1)| \; + \; |\vec{\mathbf{R}}_e(T_e) - \vec{\mathbf{R}}_1(T_1)|}{|\vec{\mathbf{R}}_k(T_k'^p) - \vec{\mathbf{R}}_e(T_{ap})| \; + \; |\vec{\mathbf{R}}_k(T_k'^p) - \vec{\mathbf{R}}_1(T_1)| \; - \; |\vec{\mathbf{R}}_e(T_e) - \vec{\mathbf{R}}_1(T_1)|}\right| \\
T^p_{grav_2} \quad &= \sum_k \frac{2fM_k}{c^3}\log\left|\frac{|\vec{\mathbf{R}}_k(T_k'^p) - \vec{\mathbf{R}}_e(T_{ap})| \; + \; |\vec{\mathbf{R}}_k(T_k'^p) - \vec{\mathbf{R}}_2(T_2)| \; + \; |\vec{\mathbf{R}}_e(T_e) - \vec{\mathbf{R}}_2(T_2)|}{|\vec{\mathbf{R}}_k(T_k'^p) - \vec{\mathbf{R}}_e(T_{ap})| \; + \; |\vec{\mathbf{R}}_k(T_k'^p) - \vec{\mathbf{R}}_2(T_2)| \; - \; |\vec{\mathbf{R}}_e(T_e) - \vec{\mathbf{R}}_2(T_2)|}\right| \\
T_2 \quad &:= T_e + \frac{1}{c}\left|\vec{\mathbf{R}}_e(T_e) - \vec{\mathbf{R}}_2(T_{2p})\right| + T_{grav_2}
\end{aligned}
\tag{20}
$$

Without a non-negligible loss of accuracy we can compute $\vec{\mathbf{R}}_k(T_k'^p)$ and $\vec{\mathbf{R}}_2(T_{2p})$ as

$$
\begin{aligned}
\vec{\mathbf{R}}_k(T_k'^p) &= \vec{\mathbf{R}}_k(T_1) \; + \; \dot{\vec{\mathbf{R}}}(T_1)\,(T_k'^p - T_1) \\
\vec{\mathbf{R}}_2(T_{2p}) &= \vec{\mathbf{R}}_2(T_2) \; + \; \dot{\vec{\mathbf{R}}}(T_2)\,(T_{2p} - T_2)
\end{aligned}
\tag{21}
$$

where $\vec{\mathbf{R}}_k(T_1)$ and $\vec{\mathbf{R}}_2(T_2)$ are computed from geocentric station coordinates using equations 3.

In general, we have to use the ephemerides of the emitter at each step of iteration in order to get its precise position at a new moment of time.

There is a special case which should be handled separately: when of the receivers is located in the geocenter, the expression for metric (1)–(2) is not valid and if used formally, a singularity occurs. It should be noted that modeling of the receiver in the geocenter does not a physical meaning, and this delay occurs only in intermediate computations. Therefore, it can be set to an arbitrary value. It is set to zero in the present algorithm.

The barycentric delay is formulated as a difference of barycentric time coordinates of events of emittance the radio wave and its receiving. However, we should remember that coordinates are not measurable quantities. They should be transformed to intervals of proper time. The VLBI time delay which emerges in analysis of fringe phases is defined as the difference of two intervals of proper time: 1) the interval of proper time of station #2 between events: coming the wave front to the reference point on the moving axis and clock synchronization; 2) the interval of proper time of station #1 between events: coming the wave front to the reference point on the moving axis and clock synchronization. The time delay is referred to the moment of coming the wave front to the reference point on the moving axis of the first antenna at time measured by the time-scale TAI. The reference point of the station for which modeling is done is defined as the point on the moving axis which has the minimal distance to the fixed axis. In the case if axes intersect, this is the point of their intersection. The differences of barycentric time coordinates $T_1 - T_{sync}$ and $T_2 - T_{sync}$ are first to transformed to geocentric coordinate system, then these differences of geocentric time coordinates are transformed to intervals of proper time using this

expression which follows from (1)–(2):

$$(t_{2p} - t_{sync}) - (t_{1p} - t_{sync}) = \left(1 - \left(\frac{U_\odot}{c^2} - L_b + \frac{V_\oplus^2}{2\,c^2}\right) - \left(\frac{U_\oplus}{c^2} - L_g + \frac{v_{1\oplus}^2}{2\,c^2}\right)\right)(T_2 - T_1) + \frac{(\vec{\mathbf{r}}_1(t_1) - \vec{\mathbf{r}}_2(t_2))\,\vec{\mathbf{V}}_\oplus}{c^2} + a + b\,(t_1 - t_{sync}) \tag{22}$$

where a and b are some quantities. Their value is irrelevant, since they cannot be distinguished from errors of clock model.

2.2 Computation of station position vector in geocentric inertial coordinate system

Time delay depends on the baricenteric position vector of the emitter and the geocentric position vector in the inertial coordinate system. The geocentric system is considered kinematicly non-rotating with respect to the barycentric coordinate system and therefore, can be labeled as a "celestial coordinate system". When we describe site position, it is convenient to relate it to the Earth crust fixed coordinate system, because in that system the motion of the antenna reference point is slow. This coordinate system is labeled as a "terrestrial coordinate system". The transformation of the position vector from the terrestrial coordinate $\vec{\mathbf{r}}_{\mathrm{T}}$ system to the celestial coordinate system $\vec{\mathbf{r}}_{\mathrm{C}}$ can be represented as

$$\vec{\mathbf{r}}_{\mathrm{C}} = \hat{\mathcal{M}}(t)\,\vec{\mathbf{r}}_{\mathrm{T}} + \vec{\mathbf{q}}(t) \times \vec{\mathbf{r}}_{\mathrm{T}} + \vec{\mathbf{d}}_{\mathrm{T}}(t) \tag{23}$$

where $\hat{\mathcal{M}}$ is the apriori rotation matrix, $\vec{\mathbf{q}}$ — the small vector of perturbing rotation, $\vec{\mathbf{d}}_{\mathrm{T}}$ — the vector of site motion the terrestrial coordinate system. The site motion can be decomposed on 1) secular motion due to plate tectonic; 2) harmonic site position variations caused by a) solid Earth tides; b) ocean loading; c) atmospheric pressure loading; d) hydrology loading; e) empirical deformations; 3) motion of the antenna reference due to antenna slewing.

2.2.1 Reduction for the Earth's rotation

Decomposition of the Earth rotation into the vector of small perturbing rotation $\vec{\mathbf{q}}(t)$ and the matrix of finite rotation $\hat{\mathcal{M}}$ is not unique, and there are different ways to perform it. The rotation vector $\vec{\mathbf{q}}(t)$ is small in the sense that one can neglect squares of its components.

Three combinations of $\vec{\mathbf{q}}(t)$ and $\hat{\mathcal{M}}$ are considered:

- Newcomb-Andoyer formalism

$$\begin{aligned} &\vec{\mathbf{q}} = 0 \\ &\hat{\mathcal{M}} = \widehat{\mathcal{R}}_3(\zeta_0) \cdot \widehat{\mathcal{R}}_2(\theta_0) \cdot \widehat{\mathcal{R}}_3(z) \cdot \widehat{\mathcal{R}}_1(-\varepsilon_0) \cdot \widehat{\mathcal{R}}_3(\Delta\psi) \cdot \widehat{\mathcal{R}}_1(\varepsilon_0 + \Delta\varepsilon) \cdot \widehat{\mathcal{R}}_3(-S) \cdot \widehat{\mathcal{R}}_2(X_p)\widehat{\mathcal{R}}_1(Y_p) \end{aligned} \tag{24}$$

- Ginot-Capitaine formalism:

$$\begin{aligned} &\vec{\mathbf{q}} = 0 \\ &\hat{\mathcal{M}} = \hat{\mathcal{R}}_3(-E) \cdot \hat{\mathcal{R}}_2(-d) \cdot \hat{\mathcal{R}}_3(E) \cdot \hat{\mathcal{R}}_3(s) \cdot \hat{\mathcal{R}}_3(-\theta) \cdot \hat{\mathcal{R}}_3(-s') \cdot \hat{\mathcal{R}}_1(Y_p) \cdot \hat{\mathcal{R}}_2(X_p) \end{aligned} \tag{25}$$

- Empirical Earth Rotation Model (EERM):

$$\vec{\mathbf{q}}(t) = \begin{pmatrix} \sum_{k=1-m}^{n-1} f_{1k}\, B_k^m(t) + \sum_j^N \Big(P_j^c \cos\omega_m t \;+\; P_j^s \sin\omega_j t\Big) \\ \qquad\qquad + t\,\Big(S_j^c \cos -\Omega_n t \;+\; S_j^s \sin -\Omega_n t\Big) \\ \sum_{k=1-m}^{n-1} f_{2k}\, B_k^m(t) + \sum_j^N \Big(P_j^c \sin\omega_j t \;-\; P_j^s \cos\omega_j t\Big) \\ \qquad\qquad + t\,\Big(S_j^c \sin -\Omega_n t \;-\; S_j^s \cos -\Omega_n t\Big) \\ \sum_{k=1-m}^{n-1} f_{3k}\, B_k^m(t) + \sum_j^N \Big(E_j^c \cos\omega_j t + E_j^s \sin\omega_j t\Big) \end{pmatrix} \tag{26}$$

$$\hat{\mathcal{M}} = \widehat{\mathcal{R}}_3(\zeta_0)\cdot\widehat{\mathcal{R}}_2(\theta_0)\cdot\widehat{\mathcal{R}}_3(z)\cdot\widehat{\mathcal{R}}_1(-\varepsilon_0)\cdot\widehat{\mathcal{R}}_3(\Delta\psi_e)\cdot\widehat{\mathcal{R}}_1(\varepsilon_0+\Delta\varepsilon_e)\cdot\widehat{\mathcal{R}}_3(-S)$$

All three approaches provide the same transformation with the same accuracy. Only two formalisms Newcomb-Andoyer and the EERM approaches are considered here.

Parameters of the Newcomb-Andoyer formalism:

$$\begin{aligned}
\zeta_0 &= \zeta_{01}\,t + \zeta_{02}\,t^2 + \zeta_{03}\,t^3 \\
\theta_0 &= \theta_{01}\,t + \theta_{02}\,t^2 + \theta_{03}\,t^3 \\
z &= z_1\,t + z_2\,t^2 + z_3\,t^3 \\
\varepsilon_0 &= \varepsilon_{00} + \varepsilon_{01}\,t + \varepsilon_{02}\,t^2 \\
\Delta\psi &= \sum_i^l \Big((\Psi_i^{pro} + \Psi'^{pro}_i T_J)\;\sin\Big(\sum_j^m k_{ji} a_j(T_J)\Big) + \\
&\qquad (\Psi_i^{ret} + \Psi'^{ret}_i T_J)\cos\Big(\sum_j^m k_{ji} a_j(T_J)\Big)\Big) + \Psi_0 + \dot{\Psi}_0 T_J + \delta\psi_{geod} \\
\Delta\varepsilon &= \sum_i^l \Big((E_{pi}^{pro} + E'^{\,pro}_{pi} T_J)\;\cos\Big(\sum_j^m k_{ji} a_j(T_J)\Big) + \\
&\qquad (E_{pi}^{ret} + E'^{\,ret}_{pi} T_J)\sin\Big(\sum_j^m k_{ji} a_j(T_J)\Big)\Big) + E_{p0} + \dot{E}_{p0} T_J + \delta\varepsilon_{geod} \\
S &= S_0 + (\Omega_n + \zeta_{01} + z_1)\,t + (\zeta_{02} + z_2)\,t^2 + (\zeta_{03} + z_3 - \frac{1}{6}\theta^2)\,t^3 \\
&\quad -(\zeta_{01} + z_1)\int_{t_o}^{t} \Delta\varepsilon(t)\,dt - \sin\varepsilon_o \int_{t_o}^{t} \Delta\psi'(t)\,\Delta\varepsilon(t)\,dt \\
&\quad +\Delta\psi\,\cos\varepsilon_0 + \kappa\mathrm{UT1}(t) \;+ A_s \;+ B_s\,t
\end{aligned} \tag{27}$$

a_j are so-called fundamental arguments represented by lower degree polynomials, The last two ad hoc spurious terms may be included for no particular reason. The geodesic nutation $\delta\psi_{geod}, \delta\varepsilon_{geod}$, is represented in the form of expansion

$$\begin{aligned}
\delta\psi_{geod} &= \sum_{i=1}^{i=6} -A_{ng}\sin(\varphi_i + (f_i + \Omega_n + z_1 + \zeta_{01} + \dot{\Psi}_0)\,t) \\
\delta\varepsilon_{geod} &= \sum_{i=1}^{i=6} \;\; A_{ng}\cos(\varphi_i + (f_i + \Omega_n + z_1 + \zeta_{01} + \dot{\Psi}_0)\,t)
\end{aligned} \tag{28}$$

The integral of cross precession-nutation and nutation-nutation terms
$-\int_{t_o}^{t} ((z_1 + \zeta_{01})\Delta\varepsilon(t) \; + \; \Delta\psi'(t)\,\Delta\varepsilon(t)\,\sin\varepsilon_o)\,dt$ have the secular and periodic terms. The secular with term truncated to the 10^{-12} rad level has a form

$$B_{nn}T_J = \frac{1}{2}\sum_{i}^{l}\sum_{j}^{m} k_{ji}\,\tfrac{\partial}{\partial t}a(T_J)\,\Psi_i^{pro}\,E_i^{pro}\,\sin\varepsilon_0\,T_J \tag{29}$$

Other periodic terms can be presented in the form

$$\rho(T_J) = \rho_c\cos(\varphi_\rho + f_\rho T_J) + \rho_s\sin(\varphi_\rho + f_\rho T_J) \tag{30}$$

To summarize, the matrix of the transformation according to the Newcomb-Andoyer formalism using the MHB2000 semi-empirical nutation expansion depends on

- 9 precession parameters: $\zeta_{0i}, \theta_{0i}, z_i$;
- 3 parameters of expansion of the angle of inclination of the ecliptic to the equator ε_{0i};
- $14 \times 3 = 42$ low degree coefficients of expansion of fundamental arguments over time;
- $14 \times 1365 = 19110$ integer multipliers k_{ij};
- $1365\Psi^{pro}$ coefficients of the prograde nutation in longitude;
- $1365\Psi'^{pro}$ coefficients of the rate of change of the prograde nutation in longitude;
- $1365\Psi^{ret}$ coefficients of the retrograde nutation in longitude;
- $1365\Psi'^{ret}$ coefficients of the rate of change of the retrograde nutation in longitude;
- $1365E^{pro}$ coefficients of the prograde nutation in obliquity;
- $1365E'^{pro}$ coefficients of the rate of change of the prograde nutation in obliquity;
- $1365E^{ret}$ coefficients of the retrograde nutation in obliquity;
- $1365E'^{ret}$ coefficients of the rate of change of the retrograde nutation in longitude;
- S_0 — nominal position angle of the Earth at J2000;
- Ω_n — nominal angular velocity of the Earth;
- B_{nn} — secular term of the nutation-nutation cross-terms;
- $6 \times 3 = 18$ phases and frequencies, and amplitudes of the geodesic nutation expansion;
- $15 \times 4 = 60$ phases and frequencies, and amplitudes of periodic nutation-precession and nutation-nutation cross terms.
- 2 spurious ad hoc terms A_s and B_s.
- κ — scaling parameter of the UT1 function

In total, 30168 parameters! In addition to that, three empirical functions UT1(t), X_p(t), and Y_p(t) describes non-predictable part of the transformation. These empirical functions are typically sampled with a step of 1 day, which requires for describing the Earth's rotation at the period of 20 years, $365 \times 3 \times 20 = 21900$ terms. The transformation in this form does not account for the free core nutation, and therefore, has the accuracy not exceeding 10^{-9}, even if empirical the functions UT1(t), X_p(t), and Y_p(t) would have been known with an infinite accuracy.

Parameters of the EERM formalism:

$$
\begin{aligned}
\zeta_0 &= \zeta_{01}\, t + \zeta_{02}\, t^2 \\
\theta_0 &= \theta_{01}\, t + \theta_{02}\, t^2 \\
z &= z_1\, t + z_2\, t^2 \\
\varepsilon_0 &= \varepsilon_{00} + \varepsilon_{01}\, t + \varepsilon_{02}\, t^2 \\
\Delta\psi &= \sum_j^3 -n_j\, \sin(\varphi_j^n + \omega_j^n\, t + \dot{\omega}_j^n\, t^2/2) \,/\, \sin\varepsilon_0 \\
\Delta\varepsilon &= \sum_j^3 \quad n_j\, \cos(\varphi_j^n + \omega_j^n\, t + \dot{\omega}_j^n\, t^2/2) \\
S &= S_0 + E_0 + (\Omega_n + \zeta_{01} + z_1 + E_1)\, t + (\zeta_{02} + z_2 + E_2)\, t^2 + \\
&\quad -(\zeta_{01} + z_1) \int_{t_o}^{t} \Delta\varepsilon(t)\, dt - \sin\varepsilon_o \int_{t_o}^{t} \Delta\psi'(t)\, \Delta\varepsilon(t)\, dt \\
&\quad +\Delta\psi\, \cos\varepsilon_0 + \sum_i^2 (E_i^c \cos\omega_i^e\, t + E_i^s \sin\omega_i^e\, t)
\end{aligned}
\tag{31}
$$

- 6 precession parameters: $\zeta_{0i}, \theta_{0i}, z_i$;
- 3 parameters of expansion of the angle of inclination of the ecliptic to the equator ε_{0i};
- $4 \times 3 = 12$ parameters of expansion of $\delta\psi$ and $\delta\varepsilon$;
- S_0 — nominal position angle of the Earth at J2000;
- Ω_n — nominal angular velocity of the Earth;
- 3 parameters of E_0, E_1, E_2 of empirical shift, drift and acceleration of the apriori E_3 Euler angle;
- B_{nn} — secular term of the nutation-nutation cross-terms;
- $5 \times 4 = 20$ phases and frequencies, and amplitudes of periodic nutation-precession and nutation-nutation cross terms.
- $3 \times 2 = 6$ frequencies and the amplitudes a priori terms of the harmonic expansion of the E_3 Euler angle.

In total, 53 parameters. The empirical function $\vec{\mathbf{q}}_e(t)$ consists of approximately 500 terms of expansion into the Fourier basis, i.e. $500 \times 5 = 2500$ parameters and 12100 parameters of the expansion into the B-spline basis over the 20 year period ($20 \times 365 \times (1 + 2/3) = 12100$), considering the time span for the B-spline basis 3 days for the first two components of the probating rotation vector $\vec{\mathbf{q}}_e(t)$ and 1 day for the third component.

Computation of station velocity and acceleration requires the first and the second time derivative of vector $\vec{q}_e$ and matrix $\hat{\mathcal{M}}$. The first derivative of the matrix $\hat{\mathcal{M}}$ is computed as

$$
\begin{aligned}
\frac{\partial}{\partial t}\hat{\mathcal{M}}(t) = \\
&\hat{\dot{\mathcal{R}}}_3(\zeta_0)\cdot\hat{\mathcal{R}}_2(\theta_0)\cdot\hat{\mathcal{R}}_3(z)\cdot\hat{\mathcal{R}}_1(-\varepsilon_0)\cdot\hat{\mathcal{R}}_3(\Delta\psi)\cdot\hat{\mathcal{R}}_1(\varepsilon_0+\Delta\varepsilon)\cdot\hat{\mathcal{R}}_3(-S)\cdot\hat{\mathcal{R}}_2(-X_p)\cdot\hat{\mathcal{R}}_3(Y_p) - \\
&\hat{\mathcal{R}}_3(\zeta_0)\cdot\hat{\dot{\mathcal{R}}}_2(\theta_0)\cdot\hat{\mathcal{R}}_3(z)\cdot\hat{\mathcal{R}}_1(-\varepsilon_0)\cdot\hat{\mathcal{R}}_3(\Delta\psi)\cdot\hat{\mathcal{R}}_1(\varepsilon_0+\Delta\varepsilon)\cdot\hat{\mathcal{R}}_3(-S)\cdot\hat{\mathcal{R}}_2(-X_p)\cdot\hat{\mathcal{R}}_3(Y_p) + \\
&\hat{\mathcal{R}}_3(\zeta_0)\cdot\hat{\mathcal{R}}_2(\theta_0)\cdot\hat{\dot{\mathcal{R}}}_3(z)\cdot\hat{\mathcal{R}}_1(-\varepsilon_0)\cdot\hat{\mathcal{R}}_3(\Delta\psi)\cdot\hat{\mathcal{R}}_1(\varepsilon_0+\Delta\varepsilon)\cdot\hat{\mathcal{R}}_3(-S)\cdot\hat{\mathcal{R}}_2(-X_p)\cdot\hat{\mathcal{R}}_3(Y_p) - \\
&\hat{\mathcal{R}}_3(\zeta_0)\cdot\hat{\mathcal{R}}_2(\theta_0)\cdot\hat{\mathcal{R}}_3(z)\cdot\hat{\dot{\mathcal{R}}}_1(-\varepsilon_0)\cdot\hat{\mathcal{R}}_3(\Delta\psi)\cdot\hat{\mathcal{R}}_1(\varepsilon_0+\Delta\varepsilon)\cdot\hat{\mathcal{R}}_3(-S)\cdot\hat{\mathcal{R}}_2(-X_p)\cdot\hat{\mathcal{R}}_3(Y_p) + \\
&\hat{\mathcal{R}}_3(\zeta_0)\cdot\hat{\mathcal{R}}_2(\theta_0)\cdot\hat{\mathcal{R}}_3(z)\cdot\hat{\mathcal{R}}_1(-\varepsilon_0)\cdot\hat{\dot{\mathcal{R}}}_3(\Delta\psi)\cdot\hat{\mathcal{R}}_1(\varepsilon_0+\Delta\varepsilon)\cdot\hat{\mathcal{R}}_3(-S)\cdot\hat{\mathcal{R}}_2(-X_p)\cdot\hat{\mathcal{R}}_3(Y_p) + \\
&\hat{\mathcal{R}}_3(\zeta_0)\cdot\hat{\mathcal{R}}_2(\theta_0)\cdot\hat{\mathcal{R}}_3(z)\cdot\hat{\mathcal{R}}_1(-\varepsilon_0)\cdot\hat{\mathcal{R}}_3(\Delta\psi)\cdot\hat{\dot{\mathcal{R}}}_1(\varepsilon_0+\Delta\varepsilon)\cdot\hat{\mathcal{R}}_3(-S)\cdot\hat{\mathcal{R}}_2(-X_p)\cdot\hat{\mathcal{R}}_3(Y_p) + \\
&\hat{\mathcal{R}}_3(\zeta_0)\cdot\hat{\mathcal{R}}_2(\theta_0)\cdot\hat{\mathcal{R}}_3(z)\cdot\hat{\mathcal{R}}_1(-\varepsilon_0)\cdot\hat{\mathcal{R}}_3(\Delta\psi)\cdot\hat{\mathcal{R}}_1(\varepsilon_0+\Delta\varepsilon)\cdot\hat{\dot{\mathcal{R}}}_3(-S)\cdot\hat{\mathcal{R}}_2(-X_p)\cdot\hat{\mathcal{R}}_3(Y_p) + \\
&\hat{\mathcal{R}}_3(\zeta_0)\cdot\hat{\mathcal{R}}_2(\theta_0)\cdot\hat{\mathcal{R}}_3(z)\cdot\hat{\mathcal{R}}_1(-\varepsilon_0)\cdot\hat{\mathcal{R}}_3(\Delta\psi)\cdot\hat{\mathcal{R}}_1(\varepsilon_0+\Delta\varepsilon)\cdot\hat{\mathcal{R}}_3(-S)\cdot\hat{\dot{\mathcal{R}}}_2(-X_p)\cdot\hat{\mathcal{R}}_3(Y_p) - \\
&\hat{\mathcal{R}}_3(\zeta_0)\cdot\hat{\mathcal{R}}_2(\theta_0)\cdot\hat{\mathcal{R}}_3(z)\cdot\hat{\mathcal{R}}_1(-\varepsilon_0)\cdot\hat{\mathcal{R}}_3(\Delta\psi)\cdot\hat{\mathcal{R}}_1(\varepsilon_0+\Delta\varepsilon)\cdot\hat{\mathcal{R}}_3(-S)\cdot\hat{\mathcal{R}}_2(-X_p)\cdot\hat{\dot{\mathcal{R}}}_3(Y_p)
\end{aligned}
\tag{32}
$$

For computing the second derivative with relative accuracy 10^{-5} it is sufficient to retain 8 terms:

$$
\begin{aligned}
\frac{\partial^2}{\partial t^2}\hat{\mathcal{M}}(t) = \\
&\hat{\mathcal{R}}_3(\zeta_0)\cdot\hat{\mathcal{R}}_2(\theta_0)\cdot\hat{\mathcal{R}}_3(z)\cdot\hat{\mathcal{R}}_1(-\varepsilon_0)\cdot\hat{\mathcal{R}}_3(\Delta\psi)\cdot\hat{\mathcal{R}}_1(\varepsilon_0+\Delta\varepsilon)\cdot\hat{\mathcal{R}}_3(-S)\cdot\hat{\mathcal{R}}_2(-X_p)\cdot\hat{\ddot{\mathcal{R}}}_3(Y_p) - \\
&2\,\hat{\dot{\mathcal{R}}}_3(\zeta_0)\cdot\hat{\mathcal{R}}_2(\theta_0)\cdot\hat{\mathcal{R}}_3(z)\cdot\hat{\mathcal{R}}_1(-\varepsilon_0)\cdot\hat{\mathcal{R}}_3(\Delta\psi)\cdot\hat{\mathcal{R}}_1(\varepsilon_0+\Delta\varepsilon)\cdot\hat{\dot{\mathcal{R}}}_3(-S)\cdot\hat{\mathcal{R}}_2(-X_p)\cdot\hat{\mathcal{R}}_3(Y_p) + \\
&2\,\hat{\mathcal{R}}_3(\zeta_0)\cdot\hat{\dot{\mathcal{R}}}_2(\theta_0)\cdot\hat{\mathcal{R}}_3(z)\cdot\hat{\mathcal{R}}_1(-\varepsilon_0)\cdot\hat{\mathcal{R}}_3(\Delta\psi)\cdot\hat{\mathcal{R}}_1(\varepsilon_0+\Delta\varepsilon)\cdot\hat{\dot{\mathcal{R}}}_3(-S)\cdot\hat{\mathcal{R}}_2(-X_p)\cdot\hat{\mathcal{R}}_3(Y_p) - \\
&2\,\hat{\mathcal{R}}_3(\zeta_0)\cdot\hat{\mathcal{R}}_2(\theta_0)\cdot\hat{\dot{\mathcal{R}}}_3(z)\cdot\hat{\mathcal{R}}_1(-\varepsilon_0)\cdot\hat{\mathcal{R}}_3(\Delta\psi)\cdot\hat{\mathcal{R}}_1(\varepsilon_0+\Delta\varepsilon)\cdot\hat{\dot{\mathcal{R}}}_3(-S)\cdot\hat{\mathcal{R}}_2(-X_p)\cdot\hat{\mathcal{R}}_3(Y_p) - \\
&2\,\hat{\mathcal{R}}_3(\zeta_0)\cdot\hat{\mathcal{R}}_2(\theta_0)\cdot\hat{\mathcal{R}}_3(z)\cdot\hat{\dot{\mathcal{R}}}_1(-\varepsilon_0)\cdot\hat{\mathcal{R}}_3(\Delta\psi)\cdot\hat{\mathcal{R}}_1(\varepsilon_0+\Delta\varepsilon)\cdot\hat{\dot{\mathcal{R}}}_3(-S)\cdot\hat{\mathcal{R}}_2(-X_p)\cdot\hat{\mathcal{R}}_3(Y_p) - \\
&2\,\hat{\mathcal{R}}_3(\zeta_0)\cdot\hat{\mathcal{R}}_2(\theta_0)\cdot\hat{\mathcal{R}}_3(z)\cdot\hat{\mathcal{R}}_1(-\varepsilon_0)\cdot\hat{\mathcal{R}}_3(\Delta\psi)\cdot\hat{\dot{\mathcal{R}}}_1(\varepsilon_0+\Delta\varepsilon)\cdot\hat{\dot{\mathcal{R}}}_3(-S)\cdot\hat{\mathcal{R}}_2(-X_p)\cdot\hat{\mathcal{R}}_3(Y_p) - \\
&2\,\hat{\mathcal{R}}_3(\zeta_0)\cdot\hat{\mathcal{R}}_2(\theta_0)\cdot\hat{\mathcal{R}}_3(z)\cdot\hat{\mathcal{R}}_1(-\varepsilon_0)\cdot\hat{\mathcal{R}}_3(\Delta\psi)\cdot\hat{\mathcal{R}}_1(\varepsilon_0+\Delta\varepsilon)\cdot\hat{\dot{\mathcal{R}}}_3(-S)\cdot\hat{\dot{\mathcal{R}}}_2(-X_p)\cdot\hat{\mathcal{R}}_3(Y_p) - \\
&2\,\hat{\mathcal{R}}_3(\zeta_0)\cdot\hat{\mathcal{R}}_2(\theta_0)\cdot\hat{\mathcal{R}}_3(z)\cdot\hat{\mathcal{R}}_1(-\varepsilon_0)\cdot\hat{\mathcal{R}}_3(\Delta\psi)\cdot\hat{\mathcal{R}}_1(\varepsilon_0+\Delta\varepsilon)\cdot\hat{\dot{\mathcal{R}}}_3(-S)\cdot\hat{\mathcal{R}}_2(-X_p)\cdot\hat{\dot{\mathcal{R}}}_3(Y_p)
\end{aligned}
\tag{33}
$$

Expression fir the first two derivatives of $\vec{q}_e$ is

$$
\vec{\dot{\mathbf{q}}}(t) = \begin{pmatrix}
m\sum\limits_{k=1-m}^{n-1} f_{1k}\,B_k^{m-1}(t) + & \sum\limits_j^N \omega_j\left(-P_j^c\sin\omega_j t \;+\; P_j^s\cos\omega_j t\right) \\
& \quad + \left(S_j^c\cos-\Omega_n t \;+\; S_j^s\sin-\Omega_n t\right) \\
& -t\,\Omega_n\left(-S_j^c\sin-\Omega_n t \;+\; S_j^s\cos-\Omega_n t\right) \\
m\sum\limits_{k=1-m}^{n-1} f_{2k}\,B_k^{m-1}(t) + & \sum\limits_j^N \omega_j\left(P_j^c\cos\omega_j t \;+\; P_j^s\sin\omega_j t\right) \\
& \quad + \left(S_j^c\sin-\Omega_n t \;-\; S_j^s\cos-\Omega_n t\right) \\
& -t\,\Omega_n\left(S_j^c\cos-\Omega_n t \;+\; S_j^s\sin-\Omega_n t\right) \\
m\sum\limits_{k=1-m}^{n-1} f_{3k}\,B_k^{m-1}(t) + & \sum\limits_j^N \omega_j\left(-E_j^c\sin\omega_j t + E_j^s\cos\omega_j t\right)
\end{pmatrix}
\tag{34}
$$

$$\vec{\ddot{\mathbf{q}}}(t) = \begin{pmatrix} m\,(m-1)\sum\limits_{k=1-m}^{n-1} f_{1k}\,B_k^{m-2}(t) \;-\; \sum\limits_{j}^{N}\omega_j^2\left(-P_j^c\cos\omega_j\,t \;+\; P_j^s\sin\omega_j\,t\right) \\ m\,(m-1)\sum\limits_{k=1-m}^{n-1} f_{2k}\,B_k^{m-2}(t) \;-\; \sum\limits_{j}^{N}\omega_j^2\left(P_j^c\sin\omega_j\,t \;-\; P_j^s\cos\omega_j\,t\right) \\ m\,(m-1)\sum\limits_{k=1-m}^{n-1} f_{3k}\,B_k^{m-1}(t) \;-\; \sum\limits_{j}^{N}\omega_j^2\left(-E_j^c\sin\omega_j\,t + E_j^s\sin\omega_j\,t\right) \end{pmatrix} \tag{35}$$

The parameterization of the Earth rotation according to the Newcomb-Andoyer representation requires knowledge of empirical functions UT1(t), $X_p(t)$, $Y_p(t)$. They are presented in the form of of time series with equal time spacing. The empirical EOP function used for data reduction are produced from analysis of observations with applying smoothing, filtering and re-sampling. Coefficients of the interpolating spline of the 3rd degree are computed using several points around the date of interest. A strong periodic signal caused by zonal tides affects function UT1(t). In order to alleviate effect of this signal in interpolation, the contribution of zonal tides to UT1 can be subtracted from the initial UT1(t) series at epochs of nodes, and then computed to the epoch of observation and added back. The contribution to UT1 caused by zonal tides can be obtained either from analysis of observations or from a a theory. In both case it is presented in the form of quasi-harmonic expansion:

$$\Delta\mathrm{UT1}(t) = \sum_i^n Z_{ci}\cos(\varphi_i + \omega_i\,t + \dot{\omega}_i\,t^2/2) + Z_{si}\sin(\varphi_i + \omega_i\,t + \dot{\omega}_i\,t^2/2) \tag{36}$$

2.3 Reduction for station secular motion

In the most general from, the reduction secular motion of an antenna can be presented in the form

$$\vec{\mathbf{r}}_{\mathrm{T}}(t) = \vec{\mathbf{r}}_0(t) \;+\; \dot{\vec{\mathbf{r}}}(t) \;+\; \sum_{k=1-m}^{n-1} F_k\,B_k^m(t) \tag{37}$$

where B_k^m is the spline of the m degree. The spline may have multiple nodes and account for the discontinuity in positions and velocities. The discontinuities may arise from either tectonic events: earthquakes or volcanic activity or be a result of a human activity, such as rail repairs. The linear part of the secular motion is caused by the plate tectonic and the isostatic glacial adjustment. The separation of the motion into linear part and expansion into the B-spline basis is entirely arbitrary.

2.4 Reduction for the displacement caused by antenna slewing

An antenna has a fixed axis A and a moving axis B (figure 1). In general, these axis do not intersect. Even if the antenna was designed to have intersecting axes, during the manufacturing process the moving axis may be shifted at 1–10 mm from the fixed axis. The antenna reference point f is the point on the fixed axis which is the closest to the moving axis. The antenna position is referred to that point. The fringe phase is referred to the phase center of the receiver that is located at the primary or secondary focus of the antenna p. During antenna slewing, position of the point b on the moving axis that is located at the point the closest of the fixed axis changes with respect to the reference point, unless the axes are perfectly intersect. We

Figure 1: Antenna axes

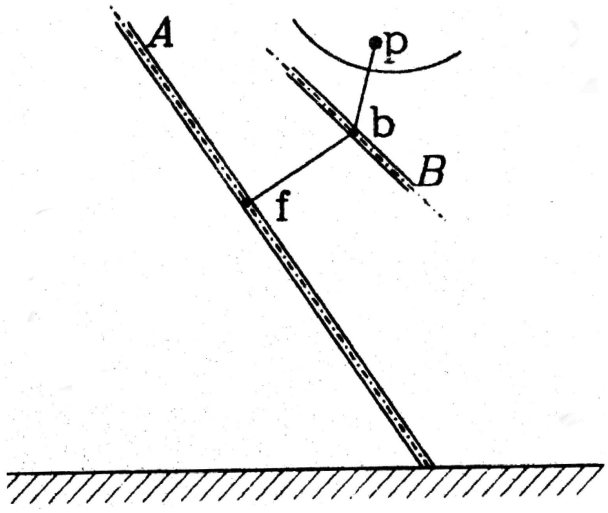

can notice that the vector $\vec{\mathbf{bp}}$ is always coincides with the source vector $\vec{\underline{\mathbf{S}}}$ during observation, therefore, the VLBI path delay for wave propagation from the point p to the point b is constant and cannot be distinguished from the clock offset. Therefore, we do not need to make reduction from the point p to the point b. However, we need to perform reduction from the point b to the point f, i.e., to compute delay for wave propagation from the point b to the point f. We will achieve it by computing the vector $\vec{\mathbf{fb}}$ in the terrestrial coordinate system and adding it to the a priori station position.

Different types of antenna mountings can be classified according to direction of the unit vector of the fix antenna $\vec{\mathbf{A}}$

- Azimuthal mounting:

$$\vec{\underline{\mathbf{a}}}_{\mathrm{U}} = \begin{pmatrix} 1 \\ 0 \\ 0 \end{pmatrix} \tag{38}$$

- Horizontal XY-N mounting:

$$\vec{\underline{\mathbf{a}}}_{\mathrm{U}} = \begin{pmatrix} 0 \\ 0 \\ 1 \end{pmatrix} \tag{39}$$

- Horizontal XY-E mounting:

$$\vec{\underline{\mathbf{a}}}_{\mathrm{U}} = \begin{pmatrix} 0 \\ 1 \\ 0 \end{pmatrix} \tag{40}$$

- Equatorial mounting:

$$\vec{\underline{\mathbf{a}}}_{\mathrm{C}} = \begin{pmatrix} 1 \\ 0 \\ 0 \end{pmatrix} \tag{41}$$

- Special case of RICHMOND

$$\vec{\underline{\mathbf{a}}}_{\mathrm{U}} = \begin{pmatrix} \cos 39^\circ 03' 36'' \cdot \cos -00^\circ 07' 12'' \\ \cos 39^\circ 03' 36'' \cdot \sin -00^\circ 07' 12'' \\ \sin 39^\circ 03' 36'' \end{pmatrix} \tag{42}$$

Subscript $_{\mathrm{U}}$ means the the vector is in the local topocentric Up-East-North coordinate system. This can be converted from to the terrestrial coordinate system through this rotation matrix transformation:

$$\vec{\mathbf{r}}_{\mathrm{T}} = \begin{pmatrix} \cos\varphi_{geod}\cos\lambda & -\sin\lambda & -\sin\varphi_{geod}\cos\lambda \\ \cos\varphi_{geod}\sin\lambda & \cos\lambda & -\sin\varphi_{geod}\sin\lambda \\ \sin\varphi_{geod} & 0 & \cos\varphi_{geod} \end{pmatrix} \vec{\mathbf{r}}_{\mathrm{U}} \tag{43}$$

The geodetic latitude φ_{geod} is computed according to [Bowring, 1985] equations:

$$\begin{aligned} \varphi_{geod} &= \operatorname{arctg} \frac{r_3(1-f_\oplus) + (2f_\oplus - f_\oplus^2)\, R_\oplus \sin^3\mu}{r_p(1-f_\oplus)(r_p - (2f_\oplus - f^2{}_\oplus)\cos^3\mu)} \\ r_p &= \sqrt{r_1^2 + r_2^2} \\ \mu &= \operatorname{arctg}\left(\frac{r_3}{r_p}\left[(1-f) + \frac{(2f_\oplus - f_\oplus^2)R_\oplus}{|r|}\right]\right) \\ h_{ort} &= r_p\cos\varphi_{geod} + r_3\sin\varphi_{geod} - R_\oplus\sqrt{1-(2f_\oplus - f_\oplus^2)\sin^2\varphi_{geod}} \end{aligned} \tag{44}$$

where $f_\oplus$ is the Earth's figure flattening and $e_\oplus$ is its eccentricity.

The vector $\vec{\mathbf{fb}}$ is expressed as

$$\vec{\mathbf{fb}} = l\frac{\vec{\underline{\mathbf{a}}} \times [\vec{\underline{\mathbf{S}}}_{app} \times \vec{\underline{\mathbf{a}}}]}{\left|\vec{\underline{\mathbf{a}}} \times [\vec{\underline{\mathbf{S}}}_{app} \times \vec{\underline{\mathbf{a}}}]\right|} = l\frac{\vec{\underline{\mathbf{S}}}_{app} - \vec{\underline{\mathbf{a}}}(\vec{\underline{\mathbf{S}}}_{app}\,\vec{\underline{\mathbf{a}}})}{|\vec{\underline{\mathbf{S}}}_{app} - \vec{\underline{\mathbf{a}}}(\vec{\underline{\mathbf{S}}}_{app}\,\vec{\underline{\mathbf{a}}})|} \tag{45}$$

where l is a parameter called "antenna axis offset", and $\vec{\underline{\mathbf{S}}}_{app}$ is an apparent source vector. The maximum value of the antenna axis offset may reach 14 meters, therefore, in order to reach 10^{-13} s accuracy in delay prediction, we need to compute vector $\vec{fb}$ with accuracy 10^{-5}. At this level of accuracy we should take into account annual aberration and refraction.

The annual aberration shifts the position vector as

$$\vec{\underline{\mathbf{s}}}_a = \frac{1}{c}\vec{\mathbf{V}}_\oplus - \frac{1}{c}(\vec{\underline{\mathbf{s}}}\,\vec{\mathbf{V}}_\oplus)\,\vec{\underline{\mathbf{s}}} \tag{46}$$

The refractively angle ρ can be computed using this expression [Sovers et al.(1998)]:

$$\rho = \frac{3.13\cdot 10^{-4}}{\operatorname{tg} E} \tag{47}$$

where E is the source elevation. Reduction for refractively is equivalent to rotation the source vector at the angle rho in the plane common to the the direction to the zenith and the source vector. Therefore, the position vector reduced for refraction is $\vec{\underline{\mathbf{s}}}_\rho = \cos\rho\,\vec{\underline{\mathbf{s}}} + \sin\rho\,\vec{\underline{\mathbf{s}}}_\perp$, where $\vec{\underline{\mathbf{s}}}_\perp$ — the vector in the plane common for the zenith vector an the vector which is perpendicular to the source vector: $\vec{\underline{\mathbf{s}}}_\perp = [\vec{\underline{\mathbf{s}}} \times \vec{\underline{\mathbf{r}}}_3] \times \vec{\underline{\mathbf{s}}}$, where $\vec{\underline{\mathbf{r}}}$ is the unit vector $\frac{\vec{\mathbf{r}}}{|r|}$.

Combining expressions 46–47, we get the following expression for the apparent source vector:

$$\begin{aligned}\underline{\vec{\mathbf{S}}}_{app} &= \frac{1}{c}\vec{\mathbf{V}}_{\oplus} - \frac{1}{c}(\underline{\vec{\mathbf{S}}}\,\vec{\mathbf{V}}_{\oplus})\,\underline{\vec{\mathbf{S}}} + \\ &\cos\left(3.13\cdot 10^{-4}\cdot\frac{\sqrt{1-\vec{\underline{\mathbf{r}}}_3\,\vec{\underline{\mathbf{S}}}}}{\vec{\underline{\mathbf{r}}}_3\,\vec{\underline{\mathbf{S}}}}\right)\underline{\vec{\mathbf{S}}} + \\ &\sin\left(3.13\cdot 10^{-4}\cdot\frac{\sqrt{1-\vec{\underline{\mathbf{r}}}_3\,\vec{\underline{\mathbf{S}}}}}{\vec{\underline{\mathbf{r}}}_3\,\vec{\underline{\mathbf{S}}}}\right)\left(\vec{\underline{\mathbf{r}}}_3 - (\vec{\underline{\mathbf{r}}}_3\,\underline{\vec{\mathbf{S}}})\underline{\vec{\mathbf{S}}}\right)\end{aligned} \tag{48}$$

Since the source vector in in the inertial coordinate system, other vectors, $\vec{\mathbf{r}}$ and $\underline{\vec{\mathbf{a}}}$ should be transformed into the inertial coordinate system before computation of $\underline{\vec{\mathbf{S}}}_{app}$.

2.5 Reduction for Earth solid tides

2.5.1 Algorithm for the computation of displacements due to solid Earth tide of the second Degree

[*Mathews et al.*(1995)] proposed the following formalism for the representation of a displacement field caused by the solid Earth tides of the second degree:

$$\vec{d}_{\text{REN}} = \sum_{m=0}^{m=2}\frac{\Phi_2^m a_e^2}{g_e}\left[\left(h^{(0)}+h^{(2)}P_2^0\right)\mathbf{R}_2^m \;+\; h'\,\mathbf{R}_0^m \;+\; \left(l^{(0)}+l^{(2)}P_2^0\right)\mathbf{S}_2^m \;+\; l^{(1)}P_1^0\,\mathbf{T}_2^m \;+\; l'\,\mathbf{T}_1^m\right] \tag{49}$$

where Φ_2^m is the tidal potential of the second degree and **R, S, T** denote radial, transverse spheroidal and toroidal vector harmonic fields:

$$\mathbf{R}_\ell^m = \vec{r}\,Y_\ell^m \qquad \mathbf{S}_\ell^m = r\,\nabla Y_\ell^m \qquad \mathbf{T}_\ell^m = i\,\vec{r}\times\nabla Y_\ell^m \tag{50}$$

here $\vec{r}$ is a unit station coordinate vector, Y_ℓ^m is a spherical harmonic function of degree ℓ and order m normalized over the unit sphere, a_e is the Earth's equatorial radius, g_e is the gravity acceleration at the equator, P_ℓ^m is a Legendre function, and h and l are the generalized Love numbers:

$h^{(0)}$ — principal Love number;
$h^{(i)}$ — out-of-phase radial Love number;
$h^{(2)}$ — latitude Love number ;
h' — zero degree Love number;
$l^{(0)}$ — principal Shida number;
$l^{(i)}$ — out-of-phase Shida number;
$l^{(1)}$ — second degree toroidal Love number;
$l^{(2)}$ — latitude Shida number;
l' — first degree toroidal Love number;

In order to transform equation (49) to the form suitable for computations we do the following operations: 1) substitute direct expressions for vector harmonic fields (50); 2) add out-of-phase terms; 3) expand the tidal potential in a Fourier time series; 4) separate the terms which depend on station latitude and longitude from the terms which depend on time. After some algebra we get the following expression for a tidal displacement vector $\vec{d}_{\mathrm{REN}}$ with radial, east and north components:

$$\vec{d}_{\mathrm{REN}} = \sum_{m=0}^{m=2} \begin{pmatrix} \vec{X}_1^{rc}(m,\varphi) \cdot \sum_{k=1}^{n(m)} A_k \, \vec{L}_1^r(k) \, \cos\gamma_{km} & - & \vec{X}_1^{rs}(m,\varphi) \cdot \sum_{k=1}^{n(m)} A_k \, \vec{L}_1^r(k) \, \sin\gamma_{km} \\ \vec{X}_2^{rc}(m,\varphi) \cdot \sum_{k=1}^{n(m)} A_k \, \vec{L}_2^r(k) \, \sin\gamma_{km} & + & \vec{X}_2^{rs}(m,\varphi) \cdot \sum_{k=1}^{n(m)} A_k \vec{L}_2^r(k) \, \cos\gamma_{km} \\ \vec{X}_3^{rc}(m,\varphi) \cdot \sum_{k=1}^{n(m)} A_k \, \vec{L}_3^r(k) \, \cos\gamma_{km} & - & \vec{X}_3^{rs}(m,\varphi) \cdot \sum_{k=1}^{n(m)} A_k \, \vec{L}_3^r(k) \, \sin\gamma_{km} \end{pmatrix} + \sum_{m=0}^{m=2} \begin{pmatrix} -\vec{X}_1^{ic}(m,\varphi) \cdot \sum_{k=1}^{n(m)} A_k \, \vec{L}_1^i(k) \, \sin\gamma_{km} & - & \vec{X}_1^{is}(m,\varphi) \cdot \sum_{k=1}^{n(m)} A_k \, \vec{L}_1^i(k) \, \cos\gamma_{km} \\ \vec{X}_2^{ic}(m,\varphi) \cdot \sum_{k=1}^{n(m)} A_k \, \vec{L}_2^i(k) \, \cos\gamma_{km} & - & \vec{X}_2^{is}(m,\varphi) \cdot \sum_{k=1}^{n(m)} A_k \, \vec{L}_2^i(k) \, \sin\gamma_{km} \\ -\vec{X}_3^{ic}(m,\varphi) \cdot \sum_{k=1}^{n(m)} A_k \, \vec{L}_3^i(k) \, \sin\gamma_{km} & - & \vec{X}_3^{is}(m,\varphi) \cdot \sum_{k=1}^{n(m)} A_k \, \vec{L}_3^i(k) \, \cos\gamma_{km} \end{pmatrix} \tag{51}$$

where vector $\vec{X}$ depends only on station coordinates:

$$\begin{aligned} \vec{X}_j^{rc}(m,\varphi) &= \vec{Z}_j^r(m,\varphi) \cdot \cos m\lambda \\ \vec{X}_j^{rs}(m,\varphi) &= \vec{Z}_j^r(m,\varphi) \cdot \sin m\lambda \\ \vec{X}_j^{ic}(m,\varphi) &= \vec{Z}_j^i(m,\varphi) \cdot \cos m\lambda \\ \vec{X}_j^{is}(m,\varphi) &= \vec{Z}_j^i(m,\varphi) \cdot \sin m\lambda \end{aligned} \tag{52}$$

here φ is geocentric latitude and λ is positive towards east longitude. Vector $\vec{Z}$ is

$$\vec{Z}_1^r = \begin{pmatrix} \bar{P}_2^m \dfrac{1}{g_e} \\ P_2^0\, \bar{P}_2^m \dfrac{1}{g_e} \\ 0 \\ \dfrac{1}{g_e} \end{pmatrix} \qquad \vec{Z}_1^i = \begin{pmatrix} \bar{P}_2^m \dfrac{1}{g_e} \end{pmatrix}$$

$$\vec{Z}_2^r = \begin{pmatrix} -\dfrac{m}{\cos\varphi}\, \bar{P}_2^m \dfrac{1}{g_e} \\ -\dfrac{m}{\cos\varphi}\, P_2^0\, \bar{P}_2^m \dfrac{1}{g_e} \\ P_1^0 \dfrac{\partial \bar{P}_2^m}{\partial\varphi} \dfrac{1}{g_e} \\ \dfrac{\partial \bar{P}_1^m}{\partial\varphi} \dfrac{1}{g_e} \end{pmatrix} \qquad \vec{Z}_2^i = \begin{pmatrix} -\dfrac{m}{\cos\varphi}\, \bar{P}_2^m \dfrac{1}{g_e} \end{pmatrix} \tag{53}$$

$$\vec{Z}_3^r = \begin{pmatrix} \dfrac{\partial \bar{P}_2^m}{\partial\varphi} \dfrac{1}{g_e} \\ P_2^0\, \dfrac{\partial \bar{P}_2^m}{\partial\varphi} \dfrac{1}{g_e} \\ -\dfrac{m}{\cos\varphi}\, P_1^0\, \bar{P}_2^m \dfrac{1}{g_e} \\ -\dfrac{m}{\cos\varphi}\, \bar{P}_1^m \dfrac{1}{g_e} \end{pmatrix} \qquad \vec{Z}_3^i = \begin{pmatrix} \dfrac{\partial \bar{P}_2^m}{\partial\varphi} \dfrac{1}{g_e} \end{pmatrix}$$

P_m^0 is a Legendre function normalized to have maximal value 1:

$$\begin{array}{lll} P_1^0 = \sin\varphi & P_1^1 = \cos\varphi & P_1^2 = 0 \\ P_2^0 = \left(\dfrac{3}{2}\sin^2\varphi - \dfrac{1}{2}\right) & P_2^1 = 2\sin\varphi\,\cos\varphi & P_2^2 = \cos^2\varphi \end{array} \tag{54}$$

and $\bar{P}_l^m$ are Legendre functions normalized over the surface of the unit sphere:

$$\begin{array}{lll} \bar{P}_1^0 = P_1^0 & \bar{P}_1^1 = P_1^1 & \bar{P}_1^2 = P_1^2 \\ \bar{P}_2^0 = \sqrt{\dfrac{5}{4\pi}}\, P_2^0 & \bar{P}_2^1 = \sqrt{\dfrac{15}{32\pi}}\, P_2^1 & \bar{P}_2^2 = \sqrt{\dfrac{15}{32\pi}}\, P_2^2 \end{array} \tag{55}$$

g_e — the Earth's equatorial gravity acceleration.

The summing in (51) is done over the constituents of the spectral expansion of the tide-generating potential which is assumed to be in the form

$$\Phi_2^m(t,r) = \sum_{m=0}^{m=2} \left(\frac{r}{a_e}\right)^2 \bar{P}_2^m(\varphi) \cdot \sum_{k=1}^{n(m)} A_k \cdot \cos\gamma_{km} \tag{56}$$

where r is the distance from the geocenter, a_e is the semi-major axis of the Earth, A_k is the normalized amplitude of the k-th tidal wave and γ_{km} is its argument:

$$\gamma_{km} = \psi_k + \theta_k + \omega_k\, t_{\rm TDB} + m\,\frac{2\pi({\rm UT1}(t) - t_{\rm TDB})}{86400} \tag{57}$$

ψ_k is the phase of the k-th wave, θ_k and ω_k are the phase and frequency of the harmonic argument of that wave. $t_{\rm TDB}$ is the time elapsed since the fundamental epoch J2000.0 (12^h 1 January, 2000) at the TDB scale. The difference ${\rm UT1} - t_{\rm TDB}$ in (57) takes into account variations in the Earth's rotation which were omitted in producing the tidal potential series. The variable m=0,1,2 in 51–53 denotes the order of a tidal wave, subscript index 1,2,3 denotes component of the displacement vector: radial, east, north, and summation is carried out over spectral harmonics of the tidal expansion. The number of constituents in sum (56), $n(m)$, is determined by a truncation level.

The vector of generalized Love numbers is presented in the form

$$\begin{array}{lcllcl} \vec{L}_1^r &=& (\,h^{(0)},\, h^{(2)},\, 0,\, h'\,)^\top & \vec{L}_1^i &=& h^{(i)} \\ \vec{L}_2^r &=& (\,l^{(0)},\, l^{(2)},\, l^{(1)},\, l'\,)^\top & \vec{L}_2^i &=& l^{(i)} \\ \vec{L}_3^r &=& (\,l^{(0)},\, l^{(2)},\, l^{(1)},\, l')^\top & \vec{L}_3^i &=& l^{(i)} \end{array} \tag{58}$$

All generalized Love numbers are considered to be complex and frequency-dependent. The generalized Love numbers are computed according to the analytical expressions presented in [*Mathews* (2001)] with corrections for some specific tidal waves taken from the tables.

The advantages of this scheme are that the sums like $\sum A_k\, \vec{L}_1^r(k)\, \sin\gamma_{km}$ depend only on time and do not depend on station coordinates, and therefore, may be used for the calculation of displacements of many stations at the same epoch. The vectors $\vec{X}$ do not depend on time and are computed only once.

The HW95 expansion contains sine and cosine coefficients C_0 and S_0. Having these coefficients, we can compute phases and amplitudes for (51) as $\psi_k = -\arctan\dfrac{S_{0k}}{C_{0k}}$ and $A_k^m = \rho(m)\sqrt{C_{0k}^2 + S_{0k}^2}$, where $\rho(m)$ is a re-normalization factor. It is $\sqrt{4\pi}$ for tides of the 0-th order and $\sqrt{8\pi}$ for other tides.

Frequencies and phases of tidal constituents are easily computed via coefficients at fundamental arguments.

$$\begin{aligned} \theta_i &= \sum_{j=1}^{j=11} k_{ij}\, F_{jo} + \theta_{ai} \\ \omega_i &= \sum_{j=1}^{j=11} k_{ij}\, F_{j1} + \omega_{ai} \end{aligned} \tag{59}$$

where F_{jq} are fundamental coefficients from the theory of planetary motion [*Simon et al.*(1994)]. We neglected terms of the 2-nd degree and higher.

2.5.2 Algorithm for the computation of displacements due to solid Earth tides of the 3-rd degree

For computation of displacements due to solid Earth tides of the 3-rd degree with a precision of 0.1mm we can neglect frequency dependence of Love numbers and an admixture of terms in tide-generating potential other than 3-rd degree as well as out-of-phase Love numbers. Therefore, vector of displacements can be written in the form

$$\vec{d}_{\rm REN} = \sum_{m=0}^{m=3} \begin{pmatrix} X_1^{3c}(m,\varphi)\, h_3 \cdot \sum\limits_{k=1}^{n(m)} A_k \cos\gamma_{km} & - & X_1^{3s}(m,\varphi)\, h_3 \cdot \sum\limits_{k=1}^{n(m)} A_k \sin\gamma_{km} \\ X_2^{3s}(m,\varphi)\, l_3 \cdot \sum\limits_{k=1}^{n(m)} A_k \sin\gamma_{km} & + & X_2^{3c}(m,\varphi)\, l_3 \cdot \sum\limits_{k=1}^{n(m)} A_k \cos\gamma_{km} \\ X_3^{3c}(m,\varphi)\, l_3 \cdot \sum\limits_{k=1}^{n(m)} A_k \cos\gamma_{km} & - & X_3^{3s}(m,\varphi)\, l_3 \cdot \sum\limits_{k=1}^{n(m)} A_k \sin\gamma_{km} \end{pmatrix} \tag{60}$$

where X depends only on station coordinates in the following way:

$$\begin{aligned} X_j^{3c}(m,\varphi) &= Z_j^3(m,\varphi) \cdot \cos m\lambda \\ X_j^{3s}(m,\varphi) &= Z_j^3(m,\varphi) \cdot \sin m\lambda \end{aligned}$$

here Z_j^3 is

$$\begin{aligned} Z_1^3(m,\varphi) &= \bar{P}_3^m \frac{1}{g_e} \\ Z_2^3(m,\varphi) &= -\frac{m}{\cos\varphi} \bar{P}_3^m \frac{1}{g_e} \\ Z_3^3(m,\varphi) &= \frac{\partial \bar{P}_3^m}{\partial\varphi} \frac{1}{g_e} \end{aligned} \tag{61}$$

Legendre functions of third order are

$$\begin{aligned} P_3^0 &= \left(\tfrac{5}{2}\sin^3\varphi - \tfrac{3}{2}\sin\varphi\right) \\ P_3^1 &= \left(\tfrac{5}{2}\sin^2\varphi - \tfrac{1}{2}\sin\varphi\right)\cos\varphi \\ P_3^2 &= \sin\varphi\cos^2\varphi \\ P_3^3 &= \cos^3\varphi \end{aligned} \tag{62}$$

$$\begin{aligned} \bar{P}_3^0 &= \sqrt{\frac{7}{4\,\pi}} P_3^0 \qquad & \bar{P}_3^1 &= \sqrt{\frac{21}{16\,\pi}} P_3^1 \\ \bar{P}_3^2 &= \sqrt{\frac{105}{32\,\pi}} P_3^2 \qquad & \bar{P}_3^3 &= \sqrt{\frac{35}{64\,\pi}} P_3^3 \end{aligned} \tag{63}$$

Analogously to the tides of the second degree, the amplitudes of the tide-generating potential produced from the HW95 expansion should be multiplied by the same re-normalization factors.

2.6 Computing displacements caused by pole tide

Earth's rotation causes the deformation of the Earth's figure. The variations in the Earth's rotation causes time variable deformations. The centrifugal potential at the point in the Earth with coordinate vector $\vec{\mathbf{r}}$ is

$$V_c = \frac{1}{2}(\vec{\mathbf{r}} \times \vec{\Omega}) \tag{64}$$

where $\vec{\Omega}$ is the vector of the Earth's angular velocity. This potential has a permanent component and the variable one. The permanent component causes a permanent displacement which cannot be observed. According to an agreement, the variable part of the centrifugal potential is determined as $V_{vc} = \frac{1}{2}(\vec{\mathbf{r}} \times \vec{\Omega}_{vc})$ where

$$\vec{\Omega}_{vc} = \Omega_n \begin{pmatrix} E_1 - E_{10} - E_{11}\, t \\ E_2 - E_{20} - E_{21}\, t \\ 1 \end{pmatrix} \tag{65}$$

where Ω_n is the nominal Earth's angular velocity and E_1, E_2, E_{11}, E_{21} are reference position of the vector of the angular velocity and its reference rate of change. Variations of third component of the vector of the Earth's angular is two order of magnitude less than the variations of the first and second component, and can be neglected. Since the dependence of the centrifugal potential with radius is the same as for the tide-generating potential, the theory of the solid Earth tides can be applied for computing displacements caused by variations of the vector of the Earth's angular velocity. Using expression 49 for tidal displacements, after simple algebra we get the following expression for displacement caused by pole tide:

$$\vec{d}_{\text{REN}} = \begin{pmatrix} h_2(\omega_{SA})\, \dfrac{\Omega_n^2\, r^2}{g_{loc}} & \Big(-\underline{r}_1\,(E_2 + E_{10} + E_{21}\, t) \;+\; \underline{r}_2\,(E_1 - E_{10} - E_{11}\, t)\Big) \\ \ell_2(\omega_{SA})\, \dfrac{\Omega_n^2\, r^2}{g_{loc}}\, \dfrac{\underline{r}_3}{\sqrt{1-\underline{r}_3^2}} & \Big(\;\underline{r}_1\,(E_1 - E_{10} - E_{11}\, t) \;+\; \underline{r}_2\,(E_2 - E_{20} - E_{21}\, t)\Big) \\ \ell_2(\omega_{SA})\, \dfrac{\Omega_n^2\, r^2}{g_{loc}}\, \dfrac{1 - 2\,\underline{r}_3^2}{\sqrt{1-\underline{r}_3^2}} & \Big(-\underline{r}_1\,(E_2 + E_{10} + E_{21}\, t) \;+\; \underline{r}_2\,(E_1 - E_{10} - E_{11}\, t)\Big) \end{pmatrix} \tag{66}$$

Love numbers are taken for the annual frequency $\omega_{SA} = 1.991 \cdot 10^{-7}$ rad s^{-1}. It should be noted, there is no unanimous agreement which parameters E_1, E_2, E_{11}, E_{21} to use in the expression 66. These parameters can be determined from fitting empirical series of $\vec{\mathbf{q}}(t)$. But since the polar motion is a stochastic process, regression parameters depend on the time period of estimation. Change in E_1, E_2, E_{11}, E_{21} will result in change of estimates of site position and velocity.

2.7 Computing displacements caused by mass loading

Displacement caused by various mass loading, ocean, atmospheric pressure, hydrology, are computed by evaluating the convolution integral over the land and over the ocean:

$$u(\vec{r}, t) = u_{\text{L}}(\vec{r}, t) + \Delta \bar{P}_o(t)\, u_o \tag{67}$$

where $\Delta\bar{P}_o(t)$ is the uniform sea-floor pressure and $u_{\rm L}(\vec{r},t)$, $u_o(\vec{r})$ are

$$\begin{aligned} u_{\rm L}(\vec{r},t) &= \sum_{i=1}^{n}\sum_{j=1}^{m} \Delta P(\vec{r}'_{ij},t)\, q(\vec{r},\vec{r}'_{ij})\, \cos\varphi_i \iint\limits_{cell_{ij}} G(\psi(\vec{r},\vec{r}'_{ij}))\, ds \\ u_o(\vec{r}) &= \sum_{i=1}^{n}\sum_{j=1}^{m} q(\vec{r},\vec{r}'_{ij})\, \cos\varphi_i \iint\limits_{cell_{ij}} G(\psi(\vec{r},\vec{r}'_{ij}))\, ds \end{aligned} \tag{68}$$

and index i runs over latitude and index j runs over longitude. Here the integration over the sphere is replaced with a sum of integrals over small cells. $q = 1$ for the vertical component.

Green's functions have a singularity in 0, so care must be taken in using numerical schemes for computing the convolution integral. Although the Green's function cannot be represented analytically over the whole range of its argument, we can always find a good approximation over a small range. We approximate the function $G(\psi)\cdot\psi$ by a polynomial of the third degree $\alpha + \beta\,\psi + \gamma\,\psi^2 + \delta\,\psi^3$. In order to compute the integral 68 over the cell, we introduce a two-dimensional Cartesian coordinate system with the origin in the center of the cell and the axis x towards east, the axis y towards north. We neglect the Earth's curvature and consider the cell as a rectangle with borders [-a, a], [-b, b] on the x and y axes respectively. Then the integral of the Green's function over the cell with respect to a site with coordinates (x_s, y_s) is evaluated analytically:

$$\iint\limits_{cell} G(\psi(x_s,y_s))\, ds = \int_{-b}^{b}\int_{-a}^{a} \left(\frac{\alpha}{\sqrt{x^2+y^2}} \;+\; \beta \;+\; \gamma\sqrt{x^2+y^2} \;+\; \delta(x^2+y^2) \right) dx\, dy =$$

$$\begin{aligned} &\left(\alpha\, y_2 + \frac{\gamma}{6}\, y_2^3\right) \ln\frac{x_2+z_{22}}{x_1+z_{12}} \;-\; \left(\alpha\, y_1 + \frac{\gamma}{6}\, y_1^3\right) \ln\frac{x_2+z_{21}}{x_1+z_{11}} \;+ \\ &\left(\alpha\, x_2 + \frac{\gamma}{6}\, x_2^3\right) \ln\frac{y_2+z_{22}}{y_1+z_{21}} \;-\; \left(\alpha\, x_1 + \frac{\gamma}{6}\, x_1^3\right) \ln\frac{y_2+z_{12}}{y_1+z_{11}} \;+ \\ &(y_2-y_1)\,(x_2-x_1)\left[\beta + \frac{\delta}{3}\left(z_{11}^2 + z_{22}^2 + x_1\,x_2 + y_1\,y_2\right)\right] \;+ \\ &\frac{\gamma}{3}\left[x_2\left(y_2\,z_{22} - y_1\,z_{21}\right) \;-\; x_1\left(y_2\,z_{12} - y_1\,z_{11}\right)\right] \end{aligned} \tag{69}$$

$$\begin{aligned} x_1 &= -a - x_s & x_2 &= \;\; a - x_s \\ y_1 &= -b - y_s & y_2 &= \;\; b - y_s \\ z_{11} &= \sqrt{x_1^2 + y_1^2} & z_{12} &= \sqrt{x_1^2 + y_2^2} \\ z_{21} &= \sqrt{x_2^2 + y_1^2} & z_{22} &= \sqrt{x_2^2 + y_2^2} \end{aligned}$$

Coordinates x_s, y_s are computed as

$$x_s = \vec{E}(\vec{r}'_{ij})\cdot\vec{T}(\vec{r}'_{ij},\vec{r}) \qquad\qquad y_s = \vec{N}(\vec{r}'_{ij})\cdot\vec{T}(\vec{r}'_{ij},\vec{r}) \tag{70}$$

where $\vec{T}(\vec{r}'_{ij},\vec{r})$ is

$$\vec{T}(\vec{r}'_{ij},\vec{r}) = \frac{\vec{r}'_{ij}\times[\vec{r}\times\vec{r}'_{ij}]}{|\vec{r}'_{ij}\times[\vec{r}\times\vec{r}'_{ij}]|} \tag{71}$$

and $\vec{E}(\vec{r}'_{ij}), \vec{N}(\vec{r}'_{ij})$ are unit vectors in east and north direction with respect to the center of the cell:

$$\vec{E}(\vec{r}'_{ij}) = \begin{pmatrix} \sin\lambda' \\ \cos\lambda' \\ 0 \end{pmatrix} \qquad \vec{N}(\vec{r}'_{ij}) = \begin{pmatrix} \sin\varphi'\cos\lambda' \\ -\sin\varphi'\sin\lambda' \\ \cos\varphi' \end{pmatrix} \tag{72}$$

It was found that when the coefficients $\alpha(\psi)$, $\beta(\psi)$, $\gamma(\psi)$ and $\delta(\psi)$ are computed with the step 0.002 rad over the range [0, 0.16] rad, and with the step 0.02 rad over the range [0.16, π], the error of the approximation of the integral 69 for a cell of size 0.044 rad (2°.5) does not exceed 1%. At large angular distances we can consider the Green's function to be constant over the cell. For an angular distance more than 0.16 rad, taking the Green's function out of the integral 68 and replacing it with the value at the angular distance between the site and the center of the cell causes an error of less than 1%.

Two land-sea masks are used for practical computation: coarse with the resolution of the surface pressure grid, and fine. If the cell of the coarse land-sea mask is completely land or completely sea, this cell is used for computing the integral 69. Otherwise, the coarse resolution cell is subdivided in smaller cells of the fine resolution grid, and the integral over each fine resolution cell is computed independently. The surface pressure is considered as defined at the corners of the coarse resolution cell. The pressure at the center of the cell is obtained by bi-linear interpolation. When $u_{\mathrm{L}}(\vec{r})$ is computed, the cells which are over ocean are bypassed. Alternatively, the cells which are over land are bypassed when $u_o(\vec{r})$ is computed.

The computation of horizontal vectors is done separately for north and east components. The north and east components of the vector $\vec{q}(\vec{r}, \vec{r}')$ are

$$\vec{q}_{\mathrm{N}}(\vec{r}, \vec{r}') = -\vec{T}(\vec{r}, \vec{r}') \cdot \vec{N}(\vec{r}) \qquad \vec{q}_{\mathrm{E}}(\vec{r}, \vec{r}') = -\vec{T}(\vec{r}, \vec{r}') \cdot \vec{E}(\vec{r}) \tag{73}$$

where $\vec{T}(\vec{r}, \vec{r}')$ is defined in a way similar to 71, but with the reverse order of arguments, $\vec{E}(\vec{r}), \vec{N}(\vec{r})$ are defined according to 72, but are the unit north and east vectors for the site under consideration.

Displacement caused by ocean tidal mass loading, non-tidal ocean mass loading, atmosphere pressure loading and hydrology loading are computed the same ways. Only the the pressure fields $\Delta P(\vec{r}'_{ij}, t)$, $\Delta \bar{P}_o P(\vec{r}'_{ij}, t)$ differ. These are empirical functions which are derived from analysis of observations.

2.8 Tropospheric path delay

Propagation medium causes an additional delay τ_m, which can be written in the form of the integral along the path l, which in general is bended:

$$\tau_m = \int (n(l) - 1) dl \tag{74}$$

Traditionally path delay τ_m in the ionosphere, the neutral equilibrium atmosphere, and in the non-equilibrium constituent of the atmosphere is considered separately. The ionosphere is a dispersive medium, so there exists a linear combination of observables at two or more frequencies which reduces the ionospheric contribution to that combination to zero. The propagation of the signal in the neutral atmosphere depends on the dependence of the refractivity with height and possibly with spatial coordinates. This dependence can be computed on the basis of the gas law for the equilibrium component, and the integral 74 can be computed analytically. It turns out, in that case the integral 74 depends only on the surface pressure and the local gravity

acceleration. The integral 74 should be computed numerically using empirical data about the global partial refractivity distribution due to the non-equilibrium constituent. Being viewed in the local topocentric coordinate system, the tropospheric path delay depends on elevation and azimuth. This can be parameterized in the form

$$\tau_{tr} = \rho_{zd} R_{zd}(E_v, A) + \rho_{zw} R_{zw}(E_v, A) \tag{75}$$

where A is the azimuth and E_v is the source elevation *ignoring* bending in the atmosphere, but taking into account annual aberration, $E_v = \arcsin(\vec{r}_{3C}\vec{\mathbf{S}}_a)$. The tropospheric path delay is split into two parts, the equilibrium (dry) and the non-equilibrium part [Davis (1985)]. Both the equilibrium and the non-equilibrium parts are presented as a product of the part which depends on ground meteorological parameters, and the dimensionless part called mapping function, which depends only on elevation and azimuth and normalized to unity in the zenith direction. Thus, the first part of the product has a meaning of zenith path delay.

In the past various expressions were proposed for the zenith path delay and the mapping function. Currently, the expression of Saastamoinen for the zenith path delay and the Niell mapping function are used. There is no evidence that alternative expressions which use ground meteorological information produce better results.

Saastamoinen expression [Saastamoinen(1972a), Saastamoinen(1972b)] for the non-equilibrium (dry) zenith path delay:

$$\begin{aligned} \rho_{zd} &= \frac{K_d\, R}{M_d\, c} \cdot \frac{P}{g_{loc} - \dfrac{\partial g}{\partial h}(0.9 h_{ort} + 7300)} \\ \rho_{zw} &= \frac{K_d\, R}{M_d\, c} \cdot \frac{1255((T\,^\circ C + 273.15) + 0.05) E_w}{g_{loc} - \dfrac{\partial g}{\partial h}(0.9 h_{ort} + 7300)} \end{aligned} \tag{76}$$

where

$K_d = 7.7604 \cdot 10^{-4}$ — dry air refractivity;

$R = 8.314742$ ($\mathrm{J} \cdot \mathrm{K}^{-1} \cdot \mathrm{mole}^{-1}$) — the universal gas constant;

$M_d = 28.9644$ — the mole mass of dry air;

c — velocity of light;

P — the surface total pressure (Pascal);

E — the surface partial pressure of water vapor (Pa);

$T\,^\circ C$ — the surface temperature (in Celsius)

g_{loc} — the local gravity acceleration;

h_{ort} — ortometric height of the antenna reference point (ref 44).

The following expression for the local gravity acceleration can be used:

$$g_{loc} = g_e \frac{1 + \dfrac{\partial g}{\partial \varphi} \sin^2 \varphi_{ast}}{\sqrt{1 - (2 f_\oplus - f_\oplus^2) \sin^2 \varphi_{geod}}} + \frac{\partial g}{\partial h} h_{ort} \tag{77}$$

where g_e — the equatorial gravity acceleration.

The absolute humidity E_w is not measured directly but deduced from observations of the of the relative humidity, i.e. the ration of the partial water vapor pressure to the pressure of the saturated water vapor at a given temperature. The following expression of [Goff & Gratch, 1946] for the pressure of the saturated water vapor E_s accepted by the International Meteorological Association can be used which is accurate to a 0.02% level:

$$\begin{aligned} \lg E_s &= 10.795\,74\left(1-\frac{T^\circ K_i}{T^\circ K}\right)- \\ &\quad 5.028\,00\lg\left(\frac{T^\circ K}{T^\circ K_i}\right)+ \\ &\quad 1.504\,75\cdot 10^{-4}\cdot\left(1-10^{-8.2969\left(\frac{T^\circ K}{T^\circ K_i}-1\right)}\right)- \\ &\quad 4.287\,3\cdot 10^{-4}\cdot\left(1-10^{-4.769\,55\left(\frac{T^\circ K}{T^\circ K_i}-1\right)}\right) \\ &\quad +2.786\,14 \end{aligned} \tag{78}$$

here $T^\circ K_i$ is the triple point of water ($T^\circ K_i = 273.^\circ 16K$).

In the case, if no pressure measurement were done at the antenna, so-called standard atmosphere of the International Meteorological Association can be used. The dependence of the atmospheric pressure on height for the standard atmosphere (table 3.9-2 in [Hrgian, 1975] can be approximated with the accuracy better 7 Pa at the height range [-700, 5500] meters using the following regression:

$$\begin{aligned} P &= 101324.2\cdot\exp(-1.1859\cdot 10^{-4}H_g - 1.1343\cdot 10^{-9}H_g^2- \\ &\quad 2.5644\cdot 10^{-14}H_g^3) \end{aligned} \tag{79}$$

where H_g is the geopotential height, which on the Earth surface can be computed as

$$H_g = \frac{9.806\,65}{g_{loc}}h_{ort} \tag{80}$$

In general the barometer is located at a different height than the antenna reference point. The air pressure at the antenna reference point differs from the air pressure of the barometer at $\Delta P = -101324.2\cdot 1.1859\cdot 10^{-4}\Delta h$.

The global Niell mapping functions [Niell (1996)] $R_d(E)$ and $R_e(E)$ are used:

$$R(E) = \frac{1+\dfrac{a}{1+\dfrac{b}{1+c}}}{\sin E+\dfrac{a}{\sin E+\dfrac{b}{\sin E+c}}}+\left(\frac{1}{\sin E}-\frac{1+\dfrac{a_t}{1+\dfrac{b_t}{1+c_t}}}{\sin E+\dfrac{a_t}{\sin E+\dfrac{b_t}{\sin E+c_t}}}\right)\cdot 10^{-3}h_{ort} \tag{81}$$

Coefficients a, b, c depends on latitude and time for the the hydrostatic mapping function, and only on latitude for the non-hydrostatic mapping function. The coefficients a_t, b_t, c_t are constants

Figure 2: Geometry of modeling residual refractivity

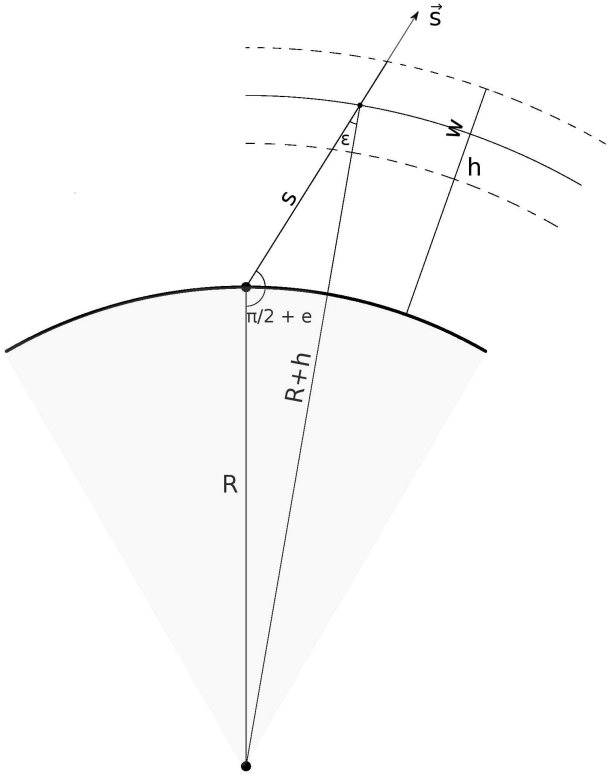

for the hydrostatic mapping function and zero for the non-hydrostatic mapping function:

$$
\begin{array}{lll}
a_h = \sum_k^7 a_{1k}\, B_k^1(|\varphi|) - \sum_k^7 a_{2k}\, B_k^1(|\varphi|)\cos(\psi_0 + \omega_{sa} t) & a_w = \sum_k^7 a_{3k}\, B_k^1(|\varphi|) & a_{ht} = \text{const} \\
b_h = \sum_k^7 b_{1k}\, B_k^1(|\varphi|) - \sum_k^7 b_{2k}\, B_k^1(|\varphi|)\cos(\psi_0 + \omega_{sa} t) & b_w = \sum_k^7 b_{3k}\, B_k^1(|\varphi|) & b_{ht} = \text{const} \\
c_h = \sum_k^7 c_{1k}\, B_k^1(|\varphi|) - \sum_k^7 c_{2k}\, B_k^1(|\varphi|)\cos(\psi_0 + \omega_{sa} t) & c_w = \sum_k^7 c_{3k}\, B_k^1(|\varphi|) & c_{ht} = \text{const}
\end{array}
\quad (82)
$$

and $a_{wt} = b_{wt} = c_{wt} = 0$. Here ω_{sa} — the angular frequency, which corresponds to the period of one year, $B_k^1(|\varphi|)$ is the B-spline of the 1st degree which depends on the absolute value of the geocentric latitude.

In a case if the distribution of residual refractivity is known, mapping function can be computed by integration. Let us consider a case when a) the *residual* atmosphere is considered uniform, i.e. its density does not depends on longitude and latitude; b) dependence of the *residual* refractivity on height h is described by a Gaussian layer model: $r(h) = r_o \exp -4\ln(2)\,(h - h_l)^2/w^2$, where h_l is the height of the layer with maximum residual refractivity and w is the full width half maximum of the distribution; c) bending in the atmosphere is neglected.

According to that model, photon propagates along slanted direction s. Within interval Δd the path delay is proportional to $r(s)ds$. The photon at at distance s has height h which by solving the triangle with sides $R, s, R + h$ in figure 2 is $h = R(\sqrt{1 + 2\sin e\, s/R + (s/R)^2} - 1)$. For the vertical direction, the integral of refractivity over the path is proportional to integral

$\int \exp\{-4\ln 2\,(h-h_l)^2/w^2\}\,dh$. Thus, the mapping function for the residual atmosphere is

$$m(e) = \frac{\int\limits_0^\infty \exp\{-4\ln 2\; R^2/w^2\;\left(\sqrt{1+2\sin e\, y+y^2}-(1+h_l/R)\right)^2\, dy\}}{\int\limits_0^\infty \exp\{4\ln 2\;(h-h_l)^2/w^2\}\,dh}, \tag{83}$$

where $y = s/R$. In practice, the limits of the integral in the denominator falls below some value ε. For instance, the expression under integral is below $1.5\cdot 10^{-5}$ outside these limits: $h_{\min} = \min(0, h_l - 2w)$, $h_{\max} = h_l + 2w$. Analogously, using the relationship between y and h by solving triangle with sides $R, s, R+h$ we find limits for the nominator:

$$y_{\min} = \sqrt{\sin^2 e + 2h_{\min}/R + (h_{min}/R)^2} - \sin e, \tag{84}$$

$$y_{\max} = \sqrt{\sin^2 e + 2h_{\max}/R + (h_{max}/R)^2} - \sin e. \tag{85}$$

2.9 Ionospheric path delay

Electromagnetic wave propagates in plasma with phase velocity

$$v_p = c\sqrt{1 - \frac{N_v\, e^2}{m_e\,\varepsilon_o\,\omega^2}} \tag{86}$$

where N_v — electron density, e — charge of an electron, m_e — mass of an electron, ε_o — permittivity of free space, ω — angular frequency of the wave and c — velocity of light in vacuum. Phase velocity in ionosphere is faster than velocity of light in vacuum.

After integration along ray path, expanding expression 86 with holding only the term of the first order, we get the following expression for additional phase rotation caused by ionosphere:

$$\Delta\varphi = -\frac{\alpha}{\omega} \tag{87}$$

where α is

$$\alpha = \frac{e^2}{2\,c\,m_e\,\varepsilon_o}\left(\int N_v\, ds_1 - \int N_v\, ds_2\right) \tag{88}$$

s_1 and s_2 are paths of wave propagation from a source to the first and second station of the radio interferometer.

If to express $\int N_v\, ds$ in units $1\cdot 10^{16}$ electrons/m^2 (so-called TEC units) then after having substituted values of constants we get

$$\alpha = 5.308018\cdot 10^{10}\ \sec^{-1}$$

A fringe phase in channel i is expressed as

$$\varphi_i = \tau_{ph}\,\omega_o + \tau_{gr}\,(\omega_i - \omega_o) - \frac{\alpha}{\omega_i} \tag{89}$$

where ω_o — is a reference sky frequency.

Unknown quantities phase and group delays: τ_{ph} and τ_{gr} can be determined from equations (89) by using weighted LSQ. Equations of conditions for such a problem can be written as

$$\tau_{ph}\frac{\partial\varphi_i}{\partial\tau_{ph}} + \tau_{gr}\frac{\partial\varphi_i}{\partial\tau_{gr}} = \varphi_i + \frac{\alpha}{\omega_i} \tag{90}$$

Actually, group and phase delays are obtained in fringing software by minimizing delay resolution function. However, it can be demonstrated that this method gives the same results as solving equations (90) by LSQ provided

- weights $\dfrac{(U_i + L_i)\,A_i}{\nu}$ are ascribed equations of conditions. U_i and L_i is the number of processed samples in upper and lower sideband of the i-th channel, A_i amplitude in this channel, ν — sampling rate.
- residual phases are not large. In practice the difference in estimates of group delay obtained by minimizing delay resolution function and by solving equations of conditions does not exceed 0.1 ps if residual phases are less than 0.4 rad (23°).

Now let's obtain explicit expression for delays by solving (89) by LSQ:

$$\hat{x} = \left((rA^\top)\,rA\right)^{-1}\,(rA^\top)\,x \tag{91}$$

where A — matrix of equations of conditions, r — vector of weights, x — vector of right parts of equations of conditions.

Partial derivatives are

$$\frac{\partial\varphi_i}{\partial\tau_{ph}} = \omega_o \qquad\qquad \frac{\partial\varphi_i}{\partial\tau_{gr}} = \omega_i - \omega_o \tag{92}$$

We can use the explicit expression for an invert of a symmetrical 2x2 matrix:

$$\begin{pmatrix} A_{11} & A_{12} \\ A_{12} & A_{22} \end{pmatrix}^{-1} = \begin{pmatrix} \dfrac{A_{22}}{\Delta} & -\dfrac{A_{12}}{\Delta} \\ -\dfrac{A_{12}}{\Delta} & \dfrac{A_{11}}{\Delta} \end{pmatrix} \qquad \Delta = A_{11}A_{22} - A_{12}^2 \tag{93}$$

We can easily find blocks of normal matrix and normal vector:

$$\begin{aligned} rA_{11} &= \omega_o^2 \sum_i^n r_i \\ rA_{12} &= \omega_o \sum_i^n r_i(\omega_i - \omega_o) \\ rA_{22} &= \sum_i^n r_i(\omega_i - \omega_o)^2 \\ \Delta &= \omega_o^2 \left(\sum_i^n r_i \cdot \sum_i^n r_i(\omega_i - \omega_o)^2 - \left(\sum_i^n r_i(\omega_i - \omega_o) \right)^2 \right) \end{aligned} \tag{94}$$

Then we can write solution of system of normal equations (92):

$$\left(\begin{array}{c}\tau_{ph}\\ \\ \tau_{gr}\end{array}\right)=\left(\begin{array}{cc}\dfrac{A_{22}}{\Delta} & -\dfrac{A_{12}}{\Delta}\\ \\ -\dfrac{A_{12}}{\Delta} & \dfrac{A_{11}}{\Delta}\end{array}\right)\left(\begin{array}{cc}\omega_o\sum\limits_i^n r_i\varphi_i & +\alpha\,\omega_o\sum\limits_i^n\dfrac{r_i}{\omega_i}\\ \\ \omega_o\sum\limits_i^n r_i(\omega_i-\omega_o)\varphi_i & +\alpha\sum\limits_i^n r_i\dfrac{\omega_i-\omega_o}{\omega_i}\end{array}\right) \tag{95}$$

or after some algebra

$$\begin{aligned}\tau_{ph}&=\frac{\sum\limits_i^n r_i(\omega_i-\omega_o)^2\cdot\sum\limits_i^n r_i\varphi_i-\sum\limits_i^n r_i(\omega_i-\omega_o)\sum\limits_i^n r_i(\omega_i-\omega_o)\varphi_i}{\omega_o\left(\sum\limits_i^n r_i\cdot\sum\limits_i^n r_i(\omega_i-\omega_o)^2-\left(\sum\limits_i^n r_i(\omega_i-\omega_o)\right)^2\right)}-\frac{\alpha}{\omega_{ph}^2}\\ \tau_{gr}&=\frac{\sum\limits_i^n r_i\cdot\sum\limits_i^n r_i(\omega_i-\omega_o)\varphi_i-\sum\limits_i^n r_i(\omega_i-\omega_o)^2\sum\limits_i^n r_i\varphi_i}{\left(\sum\limits_i^n r_i\cdot\sum\limits_i^n r_i(\omega_i-\omega_o)^2-\left(\sum\limits_i^n r_i(\omega_i-\omega_o)\right)^2\right)}+\frac{\alpha}{\omega_{gr}^2}\end{aligned} \tag{96}$$

where ω_{ph} and ω_{gr} are

$$\begin{aligned}\omega_{ph}&=\sqrt{\omega_o\frac{\sum\limits_i^n r_i\cdot\sum\limits_i^n r_i(\omega_i-\omega_o)^2-\left(\sum\limits_i^n r_i(\omega_i-\omega_o)\right)^2}{\sum\limits_i^n r_i(\omega_i-\omega_o)\sum\limits_i^n r_i\dfrac{(\omega_i-\omega_o)}{\omega_i}-\sum\limits_i^n r_i(\omega_i-\omega_o)^2\cdot\sum\limits_i^n\dfrac{r_i}{\omega_i}}}\\ \omega_{gr}&=\sqrt{\frac{\sum\limits_i^n r_i\cdot\sum\limits_i^n r_i(\omega_i-\omega_o)^2-\left(\sum\limits_i^n r_i(\omega_i-\omega_o)\right)^2}{\sum\limits_i^n r_i(\omega_i-\omega_o)^2\sum\limits_i^n\dfrac{r_i}{\omega_i}-\sum\limits_i^n r_i\cdot\sum\limits_i^n r_i\dfrac{(\omega_i-\omega_o)}{\omega_i}}}\end{aligned} \tag{97}$$

ω_{ph} and ω_{gr} are called effective ionosphere frequencies for ionosphere contribution. They have clear physical meaning: if the wide-band signal be replaced by a quasi-monochromatic signal with a group or phase effective ionosphere frequency then contribution to group or phase delay would be the same.

2.9.1 Ionosphere-free linear combinations

Using notion of ionosphere effective frequencies we can express observed group and phase delays at X and S bands through ionosphere free delay τ_{if} and parameter α:

$$\begin{aligned}\tau_{gx}&=\tau_{if}+\frac{\alpha}{\omega_{gx}^2}\\ \tau_{gs}&=\tau_{if}+\frac{\alpha}{\omega_{gs}^2}\\ \tau_{px}&=\tau_{if}-\frac{\alpha}{\omega_{px}^2}\\ \tau_{ps}&=\tau_{if}-\frac{\alpha}{\omega_{ps}^2}\end{aligned} \tag{98}$$

Here the first letter in indexes stands for group or phase delay and the second letter stands for X or S band. Using these equations we can eliminate unknown parameter α and express ionosphere free delay through a linear combination of two or three observables. The most important ionosphere-free linear combination of observables are given below:

$$\begin{aligned} \text{G\_Gxs} &= \frac{\omega_{gx}^2}{\omega_{gx}^2 - \omega_{gs}^2}\tau_{gx} - \frac{\omega_{gs}^2}{\omega_{gx}^2 - \omega_{gs}^2}\tau_{gs} \\ \text{PxGs} &= \frac{\omega_{px}^2}{\omega_{px}^2 + \omega_{gs}^2}\tau_{px} + \frac{\omega_{gs}^2}{\omega_{px}^2 + \omega_{gs}^2}\tau_{gs} \\ \text{PxGx} &= \frac{\omega_{px}^2}{\omega_{px}^2 + \omega_{gx}^2}\tau_{px} + \frac{\omega_{gx}^2}{\omega_{px}^2 + \omega_{gx}^2}\tau_{gx} \end{aligned} \tag{99}$$

Alternative way is to use expression for ionosphere contribution to group delay at X band:

$$\tau_{igx} = -\frac{\omega_{gs}^2}{\omega_{gx}^2 - \omega_{gs}^2}\left(\tau_{gx} - \tau_{gs}\right) \tag{100}$$

One can say τ_{igx} is to be added to theoretical delay and thus it will "correct" or "calibrate" group delay at X band for the ionosphere contribution. This approach is rather ugly since "calibration" or "correction" to group delay already contains this quantity (we correct observable X using the measurement of this observable itself). In order to avoid this logical pitfall is its preferable that the concept of ionosphere-free linear combinations of observables should be used.

Ionosphere frequencies vary from an experiment to experiment and they even varies during the same experiment. The table below shows typical *cyclic* ionosphere frequencies and ionosphere delays for experiment c1014 (01JUL09XA):

$$\begin{array}{rclrcl} f_{gx} &=& 8.557 \cdot 10^9 \text{ Hz} & f_{gs} &=& 2.293 \cdot 10^9 \text{ Hz} \\ f_{px} &=& 8.215 \cdot 10^9 \text{ Hz} & f_{ps} &=& 2.233 \cdot 10^9 \text{ Hz} \\ \tau_{igx} &=& 18.3\ \Delta\text{TEC ps} & \tau_{igs} &=& 255.6\ \Delta\text{TEC ps} \\ \tau_{ipx} &=& 19.9\ \Delta\text{TEC ps} & \tau_{ips} &=& 269.5\ \Delta\text{TEC ps} \end{array} \tag{101}$$

2.9.2 Ionosphere calibration using ionosphere electron contents from GPS

GPS observations are made at two frequencies, 1.2276 and 1.57542 GHz. A linear combination of two observables provides an estimate of the instantaneous TEC. Analysis of continuous GPS observations from a global network comprising 100–300 stations makes it feasible to derive an empirical model of the total electron contents over the span of observations using data assimilation technique. Such a model is routinely delivered by GPS data analysis centers since 1998. The model provides values of the TEC on a regular 3D grid. The axes of the grid are longitude, latitude, and time. The accuracy and resolution of GPS TEC model is constantly improving and is expected to improve in the future. In 2010, several analysis centers produced TEC model outputs with spatial resolution $5^\circ \times 5^\circ$ and time resolution 2 hours.

For the purpose of modeling, the ionosphere is considered as a thin spherical layer at the constant height H. Typical value of H is 450 km. In order to compute the TEC from GPS maps we need to know the coordinates of the point at which the ray pierce the ionosphere — point J in figure 3. First we find the distance from the station to the ionosphere piercing point $D = |SJ|$

Figure 3: Ray passing through the ionosphere

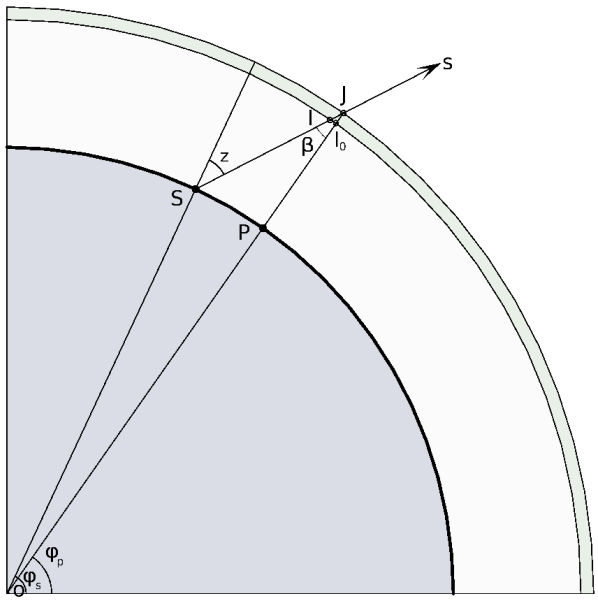

by solving triangle OSP. Noticing that $|OS| = R_\oplus$ and $|OJ| = R_\oplus + H$, we immediately get

$$\begin{aligned} \beta &= \arcsin \frac{\cos E}{1 + \dfrac{H}{R_\oplus}} \\ D &= R_\oplus \sqrt{2\frac{H}{R_\oplus}\left(1 - \sin\left(E + \beta\right)\right) + \left(\frac{H}{R_\oplus}\right)^2} \end{aligned} \tag{102}$$

Then Cartesian coordinates of point J are $\vec{r} + D\vec{s}$. Transforming them into polar coordinates geocentric latitude and longitude, we get arguments for interpolation in the 3D grid. Since the accuracy of TEC models relatively low, the choice of interpolation is irrelevant. The VTD uses 3-dimensional B-spline interpolation by expanding the TEC field into the tensor products of basic splines of the 3rd degree, although linear interpolation between the closest nodes of the grid would be sufficient. Interpolating the TEC model output, we get the TEC through the vertical path $|JI_o|$. The slanted path $|JI_1|$ is $|JI_o|/\cos\beta$. Therefore, we need to multiply the vertical TEC by $1/\cos\beta(E)$, which maps the vertical path delay through the ionosphere into the slanted path delay. Here we neglect the ray path bending in the ionosphere. We also neglect Earth's ellipticity, since the Earth was considered spherical in the data assimilation procedure of the TEC model.

Combining equations, we get the final expression for the contribution of the ionosphere to path delay:

$$\tau_{iono} = \pm \frac{\alpha}{4\,\pi^2\,f_{\text{eff}}^2}\ \text{TEC}\ \frac{1}{\cos\beta(E)} \quad , \tag{103}$$

where f_{eff} is the effective *cyclic* frequency, and sign plus is for contribution to group delay, and sign minus is for contribution to phase delay.

2.10 Delay caused by source structure

In derivation of the expression for VLBI delay we assumed that the source is point-like. In general, the complex coherence function Γ_{12} according to the Van Zitter–Zernike theorem is

$$\Gamma_{12}(b_x, b_y, \omega) = e^{i\omega\tau_0} \iint\limits_{-\infty}^{+\infty} B(x, y, \omega) e^{-2\pi i(xb_x + yb_y)/\lambda} dx\, dy \tag{104}$$

where ω is the angular reference frequency of received signal, λ is the wavelength wavelength, τ_0 — the geometric delay to the reference point on the source, B — the two-dimensional function of the brightness distribution, which depends on local Cartesian spatial coordinates x, y. These coordinates are zero in the point to which τ_0 corresponds. b_x, b_y are projection of the baseline vector $\vec{\mathbf{b}} = \vec{\mathbf{r}}_1 - \vec{\mathbf{r}}_2$ to the plane that is perpendicular to the center of the map (x=0, y=0). Integral (104) is called visibility function.

Ort $\underline{\vec{\mathbf{y}}}$ of the local Cartesian spatial coordinates related to the source position is defined as a unit vector which lies in the plane of vectors $\vec{\mathbf{S}}$ and $\underline{\vec{\mathbf{z}}}$ and is perpendicular to $\underline{\vec{\mathbf{s}}}$ (where $\underline{\vec{\mathbf{z}}}$ is the unit vector in the direction of the pole, i.e $\underline{\vec{\mathbf{z}}}_{\mathrm{T}} = (0, 0, 1)^{\top}$). Ort x is defined as the vector which is perpendicular to both $\underline{\vec{\mathbf{s}}}$ and $\underline{\vec{\mathbf{y}}}$, in such a manner that three vectors $(\vec{\mathbf{x}}, \vec{\mathbf{y}}, \underline{\vec{\mathbf{s}}})$ would form the right triplet:

$$\begin{aligned} \vec{\mathbf{x}} &= \frac{\vec{\mathbf{z}} \times \underline{\vec{\mathbf{s}}}}{|\vec{\mathbf{z}} \times \underline{\vec{\mathbf{s}}}|} \\ \vec{\mathbf{y}} &= \frac{\underline{\vec{\mathbf{s}}} \times \vec{\mathbf{x}}}{|\underline{\vec{\mathbf{s}}} \times \vec{\mathbf{x}}|} = \frac{\vec{\mathbf{z}} - \underline{\vec{\mathbf{s}}}\,(\underline{\vec{\mathbf{s}}}\,\vec{\mathbf{z}})}{|\vec{\mathbf{z}} - \underline{\vec{\mathbf{s}}}\,(\underline{\vec{\mathbf{s}}}\,\vec{\mathbf{z}})|} \end{aligned} \tag{105}$$

The phase of the coherence function is expressed as

$$\Phi = \tau_0\omega + \operatorname{arctg} \frac{\operatorname{Im} V(b_x, b_y, \omega)}{\operatorname{Re} V(b_x, b_y, \omega)} \tag{106}$$

Here we denoted the visibility function (integral in 104) with letter V. The contribution of the source structure to phase delay is the second term in 106 divided by the speed of light:

$$\tau_{ps} = \frac{1}{c} \operatorname{arctg} \frac{\operatorname{Im} V(b_x, b_y, \omega)}{\operatorname{Re} V(b_x, b_y, \omega)} \tag{107}$$

The group delay is determined as

$$\tau_{gs} = \frac{\partial}{\partial\omega} V(b_x, b_y, \omega) \tag{108}$$

We can transform expression 108 to

$$\begin{aligned} \tau_{str}(b_x, b_y) = \frac{2\pi}{c|V|^2} \Bigg[&\operatorname{Re} V(b_x, b_y) \cdot \left(\vec{\mathbf{b}}_s \overrightarrow{\operatorname{Im}\ (\nabla \mathrm{V}(\mathrm{b_x}, \mathrm{b_y}))}\right) - \\ &\operatorname{Im} V(b_x, b_y) \cdot \left(\vec{\mathbf{b}}_s \overrightarrow{\operatorname{Re}\ (\nabla \mathrm{V}(\mathrm{b_x}, \mathrm{b_y}))}\right) \Bigg] \end{aligned} \tag{109}$$

where

$$\vec{\mathbf{b}}_s = \begin{pmatrix} \vec{\mathbf{b}}\,\vec{\mathbf{x}} \\ \vec{\mathbf{b}}\,\vec{\mathbf{y}} \end{pmatrix} \qquad \overrightarrow{\nabla \mathbf{V}} = \begin{pmatrix} \dfrac{\partial}{\partial b_x} V \\ \dfrac{\partial}{\partial b_y} V \end{pmatrix} \tag{110}$$

This gives us an expression for the contribution of the source structure to group delay in the general form.

2.11 Coupling effects

There is a term τ_p, the propagation delay, in the expression for time delay 12. It is convenient to take it out the expression 12, since the propagation delay depends on meteorological parameters which cannot be predicted in advance. If we take the term τ_p out of 12, than the total delay is

$$t_2 - t_1 = (t_2 - t_1)_{geom} + \tau_p - \frac{1}{c}\vec{\mathbf{V}}_{\oplus} \cdot \vec{\underline{\mathbf{S}}}\,\tau_p \tag{111}$$

where $(t_2 - t_1)_{geom}$ is the contribution to delay without delay in the medium of propagation. The last term which give rises from the denominator in 12 is called coupling between the geometric delay and the propagation delay.

The second coupling effects give rise due to change of the height of the phase center of the receiver due to slewing as $\Delta h = \vec{\mathbf{fb}} \cdot \vec{\mathbf{r}}_{3\mathrm{C}}$. The path length through the atmosphere is changing and therefore, the tropospheric path delay. Since the expression for the zenith was referred to the reference point of the antenna, a small correction is needed. Since the tropospheric path delay is proportional to the surface pressure, $\Delta\tau_p = \tau_p \dfrac{\Delta P}{P}$. Using expression 79, we get

$$\Delta\tau_{ca} = \text{-}1.1859 \cdot 10^{-4} \left(\tau_{t1}\, \vec{\mathbf{fb}}_1 \cdot \vec{\mathbf{r}}_{1,3\mathrm{C}} - \tau_{t2}\, \vec{\mathbf{fb}}_2 \cdot \vec{\mathbf{r}}_{2,3\mathrm{C}} \right) \tag{112}$$

where $\vec{\mathbf{r}}_{1,3\mathrm{C}}$ denotes the 3rd component of the position vector in the geocentric inertial coordinate system of the 1st antenna, and $\vec{\mathbf{r}}_{1,3\mathrm{C}}$ denotes the 3rd component of the position vector of the 2nd antenna. τ_{ti} is the tropospheric path delay at the ith antenna. The additional delay 112 is called "coupling between the antenna axis and the tropospheric path delay".

3 Implementation of computation of the theoretical path delay, delay rate and partial derivatives with respect to parameters of model

The model described above is implemented in library VTD. Computation procedures is specified in the control file. The control file has the syntax of a pair keyword—`value`. The value may be either the name of the file with a priori values, or the option code, or the name of another control file. The computation procedure for delay, delay rate and partial derivatives of delays over parameters of the model has many options. Care should be taken for using options. Some options are designed for comparison tests only, some options produce correct results only if they correspond to specific a priori files.

3.1 Computation before processing the first observation

Some reduction quantities can be computed beforehand when a range of instants of observations, typically 24 hour or less, is known.

Before processing the first observation station coordinates from the input catalogue specified in the keyword STATION_COORDINATES are read. The following quantities are computed for each station: longitude, geocentric latitude, geodetic latitude, orthometric height (the hight with

respect to the reference ellipsoid), local gravity acceleration, transformation matrix from the local topocentric coordinate system Up–East–North to the Cartesian terrestrial coordinate system as well as the transformation matrix from the local topocentric coordinate system Radial–East–North to the Cartesian terrestrial coordinate system. In the first case the geodetic latitude is used in expression 43 and the second case the geocentric latitude. Time independent vectors $\vec{X}_j^{rc}(m,\varphi), \vec{X}_j^{rs}(m,\varphi), \vec{X}_j^{ic}(m,\varphi), \vec{X}_j^{is}(m,\varphi), X_j^{3c}(m,\varphi), X_j^{3s}(m,\varphi)$ which are used for computation of displacement caused by the solid Earth tides, expressions 52, 2.5.2, are computed and stored at this step.

The station motion is determined with several models. Contribution from each model is summed up.

Station linear motion is determined by velocities in the apriori file specified in the the keyword STATION_VELOCITIES. These a priori velocities are either adjusted in the VLBI solution or computed on the basis of apriori models, f.e. NUVEL if no observation at that station was made.

For each station the B-spline model of 0-th degree is defined in the file specified by the keyword STATION_ECCENTRICITIES. These are either motions of the antenna reference point with respect to the ground marker or displacements due to human activity, for instance, rail repairing, measured with a high accuracy local survey. For many stations this model is zero.

The type of antenna mounting, the length of the antenna axis offset $|\vec{\mathbf{fb}}|$ and the code of the tectonic plate where the station resides are defined in the file specified by the keyword STATION_DESCRIPTION.

Traditionally, time tags of VLBI formatters are shifted to show pseudo–UTC. The UTC is a non-differentiable function of time. It can be represented in a form of expansion over the basis of B-splines of zeroth degree. The table with epochs and amounts of jumps is specified by the keyword LEAP_SECOND. **NB:** formatter tag keeps the so-called pseudo-UTC. If the jump of UTC(t) function took place in the middle of an experiment, this jump is not applied till the end of an experiment. Therefore, in order to get a TAI instance of time that corresponds to UTC(t), one should substitute as an argument of [UTC-TAI](UTC) not the time tag at the moment of an observation, but the time tag at the moment of a nominal session start.

Position of big planets, the Sun, the Earth and the Moon are computed in accordance with numerical ephemerides using Chebyshev polynomials. Ephemerides DE403 and DE405 are supported. The file name is specified by the keyword DE_EPHEMERIDES. The argument for the numerical ephemerides is TDB. The difference $TDB - TAI(t)$ is

$$TDB(t) = TAI + \int_{t_0}^{t} \left(\frac{1}{2c^2} v^2 + \frac{U}{c^2} - L_B \right) dt + 32.184 \qquad (113)$$

This differs from 3 only by term L_B under the integral. With accuracy 10^{-5} s we can get the simplified expression for TDB:

$$TDB(t) = t \; + \; 32.184 \; + \; A_1 \sin(\varphi_{SA} + \omega_{SA} T_J) + A_2 \sin(2(\varphi_{SA} + \omega_{SA} T_J))e \qquad (114)$$

where $\omega_{SA} = 1.990968752920 \cdot 10^{-7}$ rad s^{-1} is the annual frequency, $\varphi_{SA} = 6.240076$ rad, $A_1 = 0.001658$ s, and $A_2 = 1.4 \cdot 10^{-5}$ s

3.2 Computation of the rotation matrix from the terrestrial coordinate system to the celestial coordinate system

There are several options to compute the rotation matrix which accounts for the Earth's rotation. All these options involves a sum of the secular model and coefficients of the empirical expansion.

The secular model is either analytical, or semi-analytical or empirical. It is valid for a long period of time (more than 10 years). The empirical expansion is valid for a short period of time (0.5–5.0 days). The accuracy of the resulting rotation matrix depends on accuracy of the a priori empirical expansion. There is no "good" or "bad" a priori model to the rotation matrix, but the model can be consistent or inconsistent, However, the empirical expansion was made on the basis of a certain secular model. Therefore, they both should be applied as a consistent pair. An inconsistent pair of model may potentially have very large errors. Library VTD similar to other modern astronomical reduction programs supports a wide range of options. Care should be taken to set options which are consistent.

3.2.1 IERS time series approach

In accordance to that approach parameters $\zeta_0, \theta_0, z_0, \varepsilon_0$ are computed using an expansion over low degree polynomials, $\delta\psi, \delta\varepsilon$ are computed using expansion over the quasi-harmonic basis, UT1, X_p, Y_p are computed by interpolating time series. One of the modifications of the IERS time series approach suggests using time series of expansion of empirical corrections to $\delta\psi, \delta\varepsilon$. Library VTD does not implement such a modification.

The file with time series for UT1, X_p, Y_p is specified by keyword EOP_SERIES. `EOP-MOD Ver 2.0` format of input EOP files is supported. The keyword EOP_TIME_SCALE specified by name if the argument used in that file: `TAI`, or some function of time: `TDB`, `TDT`, `UTC`, `UT1`. Coefficients of interpolating spline of the 3rd degree are computed for UT1, X_p, Y_p. An option to subtract harmonic model of variations in UT1 caused by zonal model is supported. The name of the model is specified by keyword UZT_MODEL. The following values are supported: `DICKMAN1993`, `DICKMAN1993_SHORT`, and `DICKMAN1993_PRINCIPLE` for [Dickman, 1993] model. Value `DICKMAN1993` means that all term of that model are used. Value `DICKMAN1993_SHORT` means that terms with periods less than 60 days are used. Value `DICKMAN1993_PRINCIPLE` means that 14 terms of the expansion are used, the contribution of omitted terms to UT1 rate being less than 10^{-14} rad s^{-1}. The value of the keyword UZT_USE specifies how to apply contribution to UT1 caused by zonal tides. Value `ADD` means that the contribution to UT1 will be added to function UT1 computed on the moment of observation; value `SUBTRACT` means that the contribution to UT1 will be subtracted from function UT1 computed on the moment of observation; value `INTERPOLATE` means that the contribution to UT1 will be subtracted from tabulated values of UT1 before computing coefficients of the interpolating and added back to function UT1 computed on the moment of observation.

Precession expansion is defined by keyword PRECESSION_EXPRESSION. It can have values either `LIESKE_1977` for [Lieske et al., 1976] semi-empirical low degree polynomial expansion or `CAPITAINE_2003` for low degree polynomial expansion [Capitaine et al.(2003a)].

Nutation expansion is defined by keyword NUTATION_EXPANSION. It can have the following values:

- `WAHR1980` — for Wahr 1980 expansion;
- `IERS1996` — for IERS1996 expansion;
- `REN2000` — for REN2000 expansion;
- `MHB2000` — for MHB2000 expansion;
- `MHB2000_TRANSF` — for the transfer function from the MHB2000 expansion applied to the REN2000 expansion without so-called add-on ad hoc terms;

- PETA — for the shortened version of the REN2000 expansion which comprises only of three largest terms.

Including geodesic nutation in $\Delta\psi, \Delta\varepsilon$ computation is optional and is controlled by the keyword GEODESIC_NUTATION. Value YES forces to add contribution of the geodesic nutation to nutation angles.

Computation of the rotation matrix maybe slightly altered of keyword EROT_COMPAT has value CALC10. In that case a) additional spurious terms are added to parameter S: 1) $7.07827 \cdot 10^{-8}$ — residual in the LLR solution of Chapront; 2) $-4.557249 \cdot 10^{-10}$ — accumulated difference of using UT1 instead of TAI in expression for S in the past 3) $4.462899 \cdot 10^{-20}$ T_J rad s^{-1} unknown term; $-7.220525 \cdot 10^{-20}$ T_j rad s^{-1} — spurious term introduced by N. Capitaine in order to have a symmetry in her formulae; b) terms $\delta\Psi_0$ and E_{p0} are subtracted from $\delta\Psi$ and $\delta\varepsilon$, and the rotation transformation matrix is multiplied from the left by $\hat{\mathcal{R}}_1(-\Delta\Psi_0 \sin\varepsilon_0) \cdot \hat{\mathcal{R}}_2(E_{p0}) \cdot \hat{\mathcal{R}}_3(7.07827 \cdot 10^{-8})$. This change is done for comparison tests with Calc10.

The keyword HARMONIC_EOP_FILE specified the file with empirical harmonic variations in the Earth rotation with respect to some apriori model. It compensates errors in the nutation model and omitted terms which are not forced nutations, for example, terms excited by the oceanic response and the free core nutation.

3.2.2 Earth rotation model approach

In that case instead of specifying the file with time series of X_p, Y_p, UT1, code of precession, nutation, the file with 30 coefficients of the a priori Earth rotation model is specified. The apriori model of expansion of the vector of of small perturbational rotation $\vec{\mathbf{q}}$(t) over the B-spline basis and Fourier basis can optionally be specified in keywords ERM_FILE and HARMONIC_EOP_FILE.

Typical setup when the IERS time series approach is selected

```
AEM_FILE:                NONE
ERM_FILE:                NONE
HARMONIC_EOP_FILE:       NONE
#
EOP_SERIES:              {file_name}
EOP_TIME_SCALE:          TDB
UZT_MODEL:               NONE
UZT_USE:                 NONE
PRECESSION_EXPRESSION:   CAPITAINE_2003
NUTATION_EXPANSION:      MHB2000
GEODESIC_NUTATION:       NONE
EROT_COMPAT:             NONE
```

Typical setup when the ERM approach is selected

```
AEM_FILE:                {file_name}
ERM_FILE:                {file_name}
HARMONIC_EOP_FILE:       {file_name}
#
EOP_SERIES:              NONE
EOP_TIME_SCALE:          NONE
```

```
UZT_MODEL:                NONE
UZT_USE:                  NONE
PRECESSION_EXPRESSION:    NONE
NUTATION_EXPANSION:       NONE
GEODESIC_NUTATION:        NONE
EROT_COMPAT:              NONE
```

3.3 Site displacement models

Computation of displacements caused by solid Earth tides is controlled by several keywords. The keyword SOLID_EARTH_TIDES_2ND_DEGREE specifies the name of the model for the dependence of the generalized Love numbers on frequency for the solid Earth tides of the 2nd degree, except the constituent with zero frequency. The models differ in parameters of the resonance close to the nearly diurnal free wobble and effect of anelasticity on Love numbers at low frequencies.

- `MDG97EL` — The elasticity variant of [Mathews et al., 1997] model;
- `MDG97AN` — The anelasticity variant of [Mathews et al., 1997] model;
- `DDW99EH` — The equilibrium variant of [Dehant et al., 1998] model;
- `DDW99IN` — The non-equilibrium variant of [Dehant et al., 1998] model;
- `LOVE` — Love numbers are considered to be frequency independent: $h = 0.609, l = 0.0852$;
- `MATHEWS_2000` — The variant of Mathews model as it was presented in IERS Conventions 2003;
- `MATHEWS_2001` — The variant of [*Mathews* (2001)] model'
- `NONE` — Displacements caused by solid tides are considered to be zero.

The expansion of the tide-generating potential contains terms of zero frequency. This constituents in the expansion induce the permanent displacement which is included in estimates of site position. The keyword SOLID_EARTH_TIDES_ZERO_FREQ specifies the Love number which is to be used for computing displacement due to zero-th frequency in the tide-generating potential, i.e. the permanent tide.

- `MDG97AN` — The anelastisity variant of [Mathews et al., 1997] model;
- `FLUID` — The Love numbers of the fluid limit: $h_2(\omega{=}0) = 0.94, \quad \ell_2(\omega{=}0) = 0$;
- `ZERO` — $h_2(\omega{=}0) = 0.0, \quad \ell_2(\omega{=}0) = 0.0$, i.e. the displacement vector will have only periodic terms and the zero mean.

Displacements caused by pole tide are computed using the Love numbers model specified by the keyword MPL_FILE. The supported values of this keyword are the same as for the keyword SOLID_EARTH_TIDES_2ND_DEGREE. Parameters for the linear model of components 1,2 of the perturbing vector of the Earth rotation $\vec{\mathbf{q}}$ are defined in an external file. The name of this external file is specified in the keyword MPL_FILE. Value `NONE` means that parameters E_1, E_2, E_{12}, E_{22} are zero.

Computation of displacements caused by solid Earth tides of the 3rd degree is control be keyword SOLID_EARTH_TIDES_3RD_DEGREE. Two values are supported: `NONE` and `MDG97`. Value `NONE` means that no displacements caused by tides of the 3rd degree should be computed. Value `MDG97` means that the Love numbers of the 3rd degree according to [Mathews et al., 1997] should be used.

The keyword AXIS_OFFSET_MODEL specifies whether the contribution to delay caused by motion of the receiver's phase center with respect to the antenna's reference point should be taken into account (value `YES`), or not (value `NONE`).

Displacements caused by various loading are computed by stand-alone programs. Displacements at a specific station caused by ocean loading are computed by evaluating the convolution integral 68 of the ocean tides model with appropriate Green's functions. The ocean tides model presents the complex amplitude of sea level change at a latitude/longitude grid for each harmonic constituent. The ocean tides model typically consists of 8–18 constituents. As a results of evaluating the convolution integral, complex amplitude for three components of the position vector in local topocentric coordinates system Up–East–North are computed.

Displacements at a specific station caused by the atmospheric pressure loading are computed by evaluating the convolution integral 68 and the surface atmospheric pressure field from global numerical weather models. First, the diurnal and semi-diurnal variations in surface pressure of the global atmospheric field are removed, since the atmospheric pressure variations at these frequencies in numerical weather models are corrupted, because their frequencies are close to the Nyquist frequency of the sampling input meteorological data. The semi-diurnal pressure variations are transformed to a standing wave, and the diurnal variations are folded with the ter-diurnal. Amplitudes of the diurnal and semi-diurnal signal present in the data are computed by LSQ fitting over a long time interval and subtracted from the initial pressure field fro the numerical weather mode. The convolution integral is computed separately over the land and over the sea. The actual surface pressure is used for computing the contribution to the convolution integral over the land. However under the ocean surface is deformed due to atmospheric pressure changes which should be taken into account. Currently, no reliable methods for evaluation of the oceanic response were proposed. Two extreme cases are modeled: so-called inverted barometer hypothesis which assumes that local atmospheric pressure variations are fully compensated by sea height variations, and pressure variation at the sea floor are zero, and the non-inverted barometer hypothesis which neglects sea height variations. However the inverted barometer hypothesis violates sea mass conservation. Therefore, it is modified by adding a term

$$\Delta\bar{P}_o = \frac{\iint\limits_{ocean} \Delta P(\vec{r}', t) \cos\varphi' d\lambda' d\varphi'}{\iint\limits_{ocean} \cos\varphi' d\lambda' d\varphi'} \tag{115}$$

which is applied uniformly at the sea floor. This pressure term, which depends only on time but does not depend on spatial coordinates, is used for computation of the contribution to the convolution integral over the ocean.

Since the global pressure field used for computing convolution integrals is taken from the time series of numerical weather models, the resulting displacements for stations of our interest are computed in the form of time series with the time interval of numerical weather models.

The contribution to the atmospheric pressure loading displacement caused by atmospheric tides is computed on the basis of the global model of atmospheric tides at the diurnal and semi-diurnal frequency. The complex amplitude is convolved with Green's function invoking the

non-inverted barometer hypothesis in a way similar to computing displacement caused by ocean tides.

The hydrology loading is computed in a similar way as the ocean loading: the global model of the pressure caused by stored water in land is convolved with Green's function. The resulting displacements for stations of our interest are computed in the form of time series with the time interval of hydrology models.

In addition to various mass loading, stations may have irregular displacements. These irregular displacements are estimated from analysis of VLBI observations. They are presented in the most general form: in the form of expansion over B-spline basis of an arbitrary order with non-equidistant nodes which may be multiple.

Various models of site displacements computed externally can be applied for computation of time delay. More than one external model can be used. Including these contributions to the model is controlled by the following keywords:

- POSVAR_FIL. This keyword specifies the file name with coefficients of external displacement supplied in the second value. The first value specifies the model index. The model index should be 1 for the first model, 2 for the second model, etc.
- POSVAR_MOD. This keyword specifies the type of displacement model in the second value. The first value specifies the model index. The following second values are allowed:
  - `TIME_SERIES` — the displacement model is in the form of time series which are stored in files in BINDISP format;
  - `HARMONIC_MODEL` — the displacement model is in the form of coefficients of the harmonic expansion. The model is stored in a file in HARPOS format.
  - `B_SPLINE` — the displacement model is in the form of coefficients of B-spline. The model is stored in a file in BSP format.
- POSVAR_INT — This keyword specifies the type of interpolation between nodes of displacement time series. The first value specifies the model index. The following second values are recognized:
  - `CLOSE_POINT`
  - `LINEAR`
  - `SPLINE`
- POSVAR_USE — This keyword specifies the action which is be performed in the case if no coefficients were found for a station of a baseline in the process of applying the displacement model. The first value specifies the model If the second valued is `REQUIRED`, then this situation is considered as a fatal error, and the process of computation will be terminated. If the second valued is `USE`, then a warning will be printed, but the process of computation will continue.

3.4 Computation of delay caused by propagation media. Rigorous approach.

Rigorous computation of the path delay in neutral atmosphere requires knowledge of distribution of aid temperature, atmospheric pressure and air humidity. It was shown by L. Petrov (2010, manuscript in preparation) that the atmosphere path delay can be computed with accuracies of 1–3 cm at elevation angles of 20–90° from the output of modern numerical weather models.

Rigorous computation of the atmosphere path delay requires voluminous input data (1Tb per year or more) and requires significant computing resources. It is not practical to include these computations in VTD.

Slanted path delay is computed for each station in a form of a uniform 3D series. The last dimension of the grid is time. The time step corresponds to the time step of numerical weather model (3 or 6 hours). The second dimension is azimuth and the first dimension is a function of elevation $m_i(e)$. function $m_i(e)$ is the so-called "mapping function" for the ISO atmosphere: $\frac{t_{na}(e)}{t_{na}(\pi/2)}$ — the ratio of the atmosphere path delay at a given direction to the atmosphere path delay in zenith direction computed for the reference model of the atmosphere ISO ISA at geoid at the latitude 45°. Function $m_i(e)$ is computed by numerical integration of equations of wave propagation, and is represented in the form of $m_i(e) = \sum C_k T_k((\frac{1}{\sin e + \alpha} - a)/b)$ where $T_k(x)$ is the Chebyshev polynomial of the k-th degree, a, b, α, C_k are some coefficients. The function reciprocal to $m(e)$, $m^{-1}(r)$, is represented as $m^{-1}(r) = -\alpha + \arcsin(1/\sum D_k T((r-c)/d))$.

Interpolation of the slated path delay $\tau_{na}(e, A, t)$ is performed by the following way. First, for the range of epochs within observing session (3 epochs before the experiment start and 3 epochs after the experiment, each station the 3D array of slanted path delay for dimensions $r, A, t(r = m_i(e)$ is extracted. Then the 3D array of B-spline coefficients that represents the slanted path delay is computed on place and replaces the array of 3D path delay.

Finally, the slanted path delay at elevation e, azimuth A at time epoch t is computed using these interpolation B-spline coefficients as a function (r, A, t). Coordinate $r = m_i(e)$. The partial derivative of the slanted path delay with respect to the path delay in zenith direction $\frac{\tau_{na}(e)}{\tau_{na}(\pi/2)}$ is computed as $\frac{\tau_{na,nh}(e)}{\tau_{na,nh}(\pi/2)}$, where $\tau_{na,nh}(e)$ is the contribution of the non-hydrostatic constituent of the atmosphere on path delay.

3.4.1 Computation of path delay through the neutral atmosphere using the output of numerical weather models.

Numerical whether models produces the 4D field of the atmospheric pressure, air temperature, specific humidity, and other parameters on a non-regular, global 4D grid. For computing path delay, the non-regular grid is replaced with the regular grid through re-gridding and the use of curvilinear coordinate. The curvilinear coordinates H, L, P, T are related to the Cartesian, crust-fixed coordinates x, y, z, t through the matrix of transformation $\hat{\mathcal{H}}$, such that $R(H, \vec{L}, P, T) = \hat{\mathcal{H}} r(x, \vec{y}, z, t)$. The coefficients of the transformation $\hat{\mathcal{H}}$ are global and do not depend on coordinates.

For a given station, local Cartesian coordinates ξ, η, ζ with the original ant the station reference point are introduced, such that the direction of axis ξ is along the direction to the emitter, as it were in the absence of the atmosphere, η is the perpendicular to ξ an lies in the plane of ξ and the Earth pole, and $\zeta = \xi \times \zeta$. It was shown by L. Petrov 2010, paper in preparation, that exploiting the Fermat principle and solving the variational problem for finding the trajectory through the heterogeneous atmosphere, the differential equations of wave propagation can be written in this form:

$$\begin{aligned} \frac{d^2\eta}{d\xi^2} + \frac{n_\xi}{n}\frac{d\eta}{d\xi} &= \frac{n_\eta}{n} + U(n, n_\xi, n_\eta, n_\zeta, \frac{d\eta}{d\xi}, \frac{d\zeta}{d\xi}, \frac{d^2\zeta}{d\xi^2}) \\ \frac{d^2\zeta}{d\xi^2} + \frac{n_\xi}{n}\frac{d\zeta}{d\xi} &= \frac{n_\zeta}{n} + V(n, n_\xi, n_\eta, n_\zeta, \frac{d\eta}{d\xi}, \frac{d\zeta}{d\xi}, \frac{d^2\zeta}{d\xi^2}) \end{aligned} \tag{116}$$

where U and V gather non-linear terms that can be omitted if elevations are greater than 3° and the accuracy of computation 1 ps is considered sufficient. Here n is the refractivity coefficient that is computed on the basis of the atmospheric pressure, air temperature and specific humidity as

$$n = 1 + k_{1d}\frac{P_d}{T}Z_d^{-1} + \left(k_{1w}\frac{P_w}{T} + k_{2w}\frac{P_w}{T^2}\right) Z_w^{-1}, \tag{117}$$

After numerical solving differential equations (116), functions $\eta(\xi), \zeta(\xi), \eta'(\xi), \zeta'(\xi)$ become known. Then the slanted path delay is found by integration of the refractivity index along the curvilinear trajectory $\eta(\xi), \zeta(\xi)$:

$$\tau_{na} = \frac{1}{c}\int_0^\infty \left(n\left(\xi, \eta, \zeta\right) \sqrt{1 + \left(\frac{d\eta}{d\xi}\right)^2 + \left(\frac{d\zeta}{d\xi}\right)^2} - 1 \right) d\xi. \tag{118}$$

Computation of the path delay through the neutral atmosphere is a computationally intensive process are requires voluminous dataset (1Tb per year). Therefore, for practical reasons, the slanted path delay is computed outside of VTD. The slanted path delay is computed for each site, each time epoch of the numerical weather model by first solving differential equations 117 and then integrating the refractivity index along the trajectory at a 2D grid: azimuth and elevation. In order to exploit efficient interpolation, the grid should be equidistant. Since the dependence of path delay on elevation is strongly non-linear, equidistant grid over azimuth and elevation is the not the optimal: in order to get interpolation errors below 1 ps, too many nodes over elevation are needed. The efficiency of interpolation is significantly improved if to perform a non-linear transformation of the grid, i.e. to present the slanted path delay on a regular grid of arguments others than azimuth and elevation. The optimal choice is a function that represents the average path delay. Numerical experiments show that a satisfactory approximation is achieved when when we transform arguments $(A, E) \longrightarrow (A, M_{\rm iso}(P(E)))$, where A stands for azimuth, E for elevation, and $M_{\rm st}(P(E))$ is the mapping function computed for the refractivity index distribution determined by the ISO International Standard Atmosphere [ISO (1975)]. This function itself is represented not as a function of elevation but as a function of another, more simple, approximation of the mapping function, namely

$$P(E) = \frac{1}{E\left(1 + \frac{2}{\pi}E_0\right) - E_0} \quad , \tag{119}$$

where E_0 is -0.052 radians is selected in such a way that to avoid singularity even for the ray grazing the horizon and remain normalized to 1 in zenith direction. Series of expansion $M_{\rm st}(P(E))$ are converging much faster than series $M_{\rm st}(P(E))$. Function $M_{\rm st}(P(E))$ was first

computed by numerical integration at the range of elevations $[-0.052, \frac{\pi}{2}]$ at a regular elevation grid of size 1024. Then the series of $M_{\rm st}(P(E))$ were expanded over Chebyshev polynomial of the 12th degree:

$$\begin{aligned} M_{\rm st}(P(E)) &= \sum_{n=0}^{n=12} c_n\, T_n\left(\frac{P(E)-P_b}{P_e-P_b}\right) \\ M_{\rm st}^{-1}(M) &= \frac{1}{1+\frac{2}{\pi}E_0}\ \arcsin\frac{1}{\left(\sum_{n=0}^{n=12} d_n\, T_n\left(\frac{M-M_b}{M_e-M_b}\right)\right)}, \end{aligned} \tag{120}$$

where $P_b = -0.052$, $P_e = \frac{\pi}{2}$ and $M_b = 1.0$, $M_e = 46.815214$. The inverse $M_{\rm st}^{-1}(M)$ returns elevation angle as a function of mapping function.

Numerical values of Chebyshev polynomial coefficients of $M_{\rm st}(P(E))$ and its inverse $M_{\rm st}^{-1}(M)$ are presented in table 1.

Table 1: The second column presents the coefficients of expansion of mapping function for the International Standard Atmosphere as a function of P(E) over Chebyshev polynomials at the range of elevations $[-0.052, \frac{\pi}{2}]$. The third column presents the coefficients of expansion of its inverse $M_{\rm st}^{-1}(M)$ over Chebyshev polynomials at the range $[1.0, 46.815214]$. The argument of the inverse is the mapping function, and the value is elevation. The maximal error of interpolation is $8 \cdot 10^{-6}$.

Deg	$M_{\rm st}(P(E))$	$M_{\rm st}^{-1}(M)$
0	$2.3496276 \cdot 10^{+01}$	$1.433399 \cdot 10^{+01}$
1	$2.3756641 \cdot 10^{+01}$	$1.255039 \cdot 10^{+01}$
2	$2.8960727 \cdot 10^{-01}$	$-1.159927 \cdot 10^{-01}$
3	$-8.8489567 \cdot 10^{-01}$	$4.812282 \cdot 10^{-01}$
4	$1.4212949 \cdot 10^{-01}$	$-1.142513 \cdot 10^{-01}$
5	$3.4080806 \cdot 10^{-02}$	$4.717299 \cdot 10^{-02}$
6	$-2.1776292 \cdot 10^{-02}$	$-1.584444 \cdot 10^{-02}$
7	$2.6966697 \cdot 10^{-03}$	$5.871918 \cdot 10^{-03}$
8	$1.3182015 \cdot 10^{-03}$	$-1.949435 \cdot 10^{-03}$
9	$-9.2308499 \cdot 10^{-04}$	$7.900266 \cdot 10^{-04}$
10	$6.8354478 \cdot 10^{-05}$	$-2.467537 \cdot 10^{-04}$
11	$1.3502649 \cdot 10^{-05}$	$9.892615 \cdot 10^{-05}$
12	$-1.7105554 \cdot 10^{-05}$	$-1.280538 \cdot 10^{-04}$

Numerical experiments showed that the interpolation errors are below 1 ps at elevations $[3^\circ, 90^\circ]$ when the slanted path delay at a given station is expanded over B-spline basis at a regular grid $A, M_{\rm st}(P(E))$ with 12 steps over azimuth in the range of $[0, 2\pi]$ and 16 steps over $M_{\rm st}(P(E))$ in the range of [1.0, 14.65859].

In order to interpolate slanted path delay at A, E, T (T is time), the triplet of arguments should be transformed to A, M, T using expression 120. The 3D field of slanted path delay at a

given station is expanded over B-spline series of the m-th degree:

$$\tau_{\rm na}(A,M,T) = \sum_{l=1-m}^{l=d_T} \sum_{k=1-m}^{k=d_M} \sum_{j=1-m}^{j=d_A} f_{ijk}\, B_i^m(A)\, B_j^m(M)\, B_k^m(T) \quad . \tag{121}$$

Interpolation of slanted path delay and applying it to the total path delay in VTD is controlled by keywords SLANTED_PATH_DELAY_MODEL, SLANTED_PATH_DELAY_BIAS_FILE, EXTERNAL_DELAY_DIR, EXTERNAL_DELAY_DIR_2ND, EXTERNAL_DELAY_DIR_3RD, and EXTERNAL_DELAY_DIR_4TH.

The first keyword is either NONE or SPD_3D. The latter values indicates that the 3D slanted path delay should be read from external files and interpolated. The files with path delay are located up to 4 directories, one file per station. VTD will look first directory EXTERNAL_DELAY_DIR, then EXTERNAL_DELAY_DIR_2ND, then EXTERNAL_DELAY_DIR_3RD, and at lastEXTERNAL_DELAY_DIR_4TH. If more than one file for a given station is provided, the file from the first directory will be picked up.

Slanted path delay can be corrected for station-dependent empirical additive offset a and multiplicative bias b:

$$\tau_{\rm na} = \tau_{\rm na-orig} + a_{\rm offset} + b\,\tau_{\rm nhy-orig} \quad , \tag{122}$$

where $\tau_{\rm nhy-orig}$ is original non-hydrostatic component of the path delay through the neutral atmosphere. Keyword SLANTED_PATH_DELAY_BIAS_FILE specifies the name of that file. If it NONE, no empirical correction is made.

3.4.2 Computation of path delay through the neutral atmosphere. Regression approach.

In the absence of rigorous computations, the path delay can be evaluated as

$$\tau_{atm} = \tau_{hz}\, m_h(e + \eta\cos(A) + \varepsilon\sin(A)) + \tau_{nz}\, m_n(e + \eta\cos(A) + \varepsilon\sin(A)) \tag{123}$$

where τ_{hz} — is the hydrostatic constituent of the path delay in the neutral atmosphere in zenith direction, τ_{nz} — is the the non-hydrostatic constituent of the path delay the neutral atmosphere in zenith direction, $m_h(e)$ and $m_n(e)$ are the so-called mapping functions that describe the dependence of the atmosphere path delay on the angle between the source and the symmetry axis of the atmosphere. e are A the elevation angle and the azimuth in vacuum, η and ε are inclination angles of the symmetry axis in the north and east directions.

Hydrostatic constituent of the path delay in zenith direction can be computed using the atmospheric pressure at the level of the reference point with accuracy 2–5 ps. Other parameters of 123 cannot be predicted without detail knowledge of the atmospheric parameters profile. Therefore, a regression expression is used. The most precise regression expression was computed using the output of the numerical weather model GEOS–5. Regression coefficients were computed for all 205 VLBI stations.

Computation of the hydrostatic path delay in the source direction is controlled by two options: HYDROSTATIC_ZENITH_DELAY and HYDROSTATIC_MAPPING_FUNCTION. The keyword HYDROSTATIC_ZENITH_DELAY support values `NONE`, `SAASTAMOINEN` for the model of [Saastamoinen(1972a), Saastamoinen(1972b)], or MMF for the Mean Mapping Function Model (L. Petrov (2009), manuscript in preparation). Saastamoinien model is the best model. No hydrostatic path delay is computed when keyword HYDROSTATIC_ZENITH_DELAY has value `NONE`. The zenith path delay is to be multiplied by the mapping function which is defined in

the keyword HYDROSTATIC_MAPPING_FUNCTION. The alternatives are `NMFH` for the Niell hydrostatic mapping function and MMF for the Mean Mapping Function.

Computation of the non-hydrostatic, wet path delay in the source direction is controlled by two options: WET_ZENITH_DELAY and WE_MAPPING_FUNCTION. The keyword WET_ZENITH_DELAY support values MMF for the Mean Mapping Function Model, and `NONE`. In the latter case no wet path delay is computed. The MMF is the best model. The zenith path delay is to be multiplied by the mapping function which is defined in the keyword WET_MAPPING_FUNCTION. Alternatives are `NMFW` for the Niell non-hydrostatic mapping function and MMF for the Mean Mapping Function.

Computation of path delay depends on surface meteorological parameters. In the absence of measured meteorological parameters, default values are computed on the basis of the model specified by the keyword METEO_DEF. If the value of pressure are out of range [500 00, 110 000] Pa, all meteorological parameters, air pressure, air temperature and relative humidity are considered missing. Three values are supported `IMA`, `CALC` and `NONE`. The value `IMA` means if the surface meteorological parameters are missing they are computed according to the model of the International Meteorological Association. The value `CALC` means that the surface meteorological parameters are computed in the mode of compatibility with Calc: $P = 101325.0D0 \cdot (1 - 6.5 \cdot 10^{-3} \cdot h_{ort}/293.15)^{5.26}$. The origin of the model that Calc uses is obscure. The value `NONE` means that any value of pressure, temperature and relatives are considered present, regardless whether they are out of range or not.

3.4.3 Computation of delay ionosphere path delay.

Keyword IONOSPHERIC_MODEL specifies whether ionosphere path delay is to be computed. Supported values: NONE or GNSS_TEC_MAP. Value GNSS_TEC_MAP means that ionosphere path delay will be computed using gridded time series of TEC from analysis of global navigation satellite systems, such as GPS or GLONASS. The files with the TEC values in VIONO format are specified by keywords IONOSPHERE_DATA_FILE, IONOSPHERE_DATA_FILE_2ND IONOSPHERE_DATA_FILE_3RD, IONOSPHERE_DATA_FILE_4TH. Why more than one file? The data file is supposed to present TEC at a regular grid with the same step, without gaps. The TEC model may have different grid size and may have gaps. In that case the dataset is split into several files, each of them presents the TEC model at a regular grid without gaps. If more than one TEC model outputs are specified in keywords IONOSPHERE_DATA_FILE, IONOSPHERE_DATA_FILE_2ND IONOSPHERE_DATA_FILE_3RD, IONOSPHERE_DATA_FILE_4TH, then it is assumed that each file covers different time span.

3.5 Partial derivatives and coupling effects.

Partial derivatives of time delay and delay rate with respect to parameters of the product of the tilt of the symmetry axis of the atmosphere in the local topocentric coordinate system and the zenith path delay are computed in accordance with the expression specified by the keyword ATMOSPHERE_TILT_PARTIALS. The following values are supported:

- `MACMILLAN_1995` — Expression according to [McMillan and Ma (1997)]:

$$\frac{\partial \tau}{\partial \tau_{grad,North}} = R_{zd}\frac{\cos A}{\tan E} \tag{124}$$

$$\frac{\partial \tau}{\partial \tau_{grad,East}} = R_{zd}\frac{\sin A}{\tan E} \tag{125}$$

- TILT_NMFH — Expression according to [Chen and Herring (1997)]:

$$\frac{\partial \tau}{\partial \tau_{grad,North}} = R_{zd} \frac{\cos A}{\tan E \sin E + C} \tag{126}$$

$$\frac{\partial \tau}{\partial \tau_{grad,East}} = R_{zd} \frac{\sin A}{\tan E \sin E + C} \tag{127}$$

- TILT_NMFW — Expression according to [Chen and Herring (1997)]:

$$\frac{\partial \tau}{\partial \tau_{grad,North}} = R_{zw} \frac{\cos A}{\tan E \sin E + C} \tag{128}$$

$$\frac{\partial \tau}{\partial \tau_{grad,East}} = R_{zw} \frac{\sin A}{\tan E \sin E + C} \tag{129}$$

- NONE — No partial derivative with respect to parameters of the tilt to perform.

where $C = 0.0031$.

Computation of the coupling term between the tropospheric path delay and axis offset is controlled by the keyword TROP_AXOF_COUPLING, which supports two values: YES and NONE. Computation of the coupling term between the tropospheric path delay and the geometric delay is controlled by the keyword TROP_GEOMETRIC_COUPLING, which supports two values: YES and NONE.

Computation of delay rate using an analytical expression can be turned on or turned off in accordance with the value of the keyword DELAY_RATE: YES or NONE.

Keywords GEOM_EXPR_FAR_ZONE, GEOM_EXPR_FAR_ZONE, and SOURCE_STRUCTURE are reserved for future. Currently, they should have the following values:

- GEOM_EXPR_FAR_ZONE PK2001
- GEOM_EXPR_FAR_ZONE LIGHT_TIME
- SOURCE_STRUCTURE NONE

The keyword GRS_METRIC specifies the scaling parameter in the metric tensor for the geocentric coordinate system. The following values are supported:

- ITRF2000 — The ITRF2000 metric (the same as IERS1992): $L_g = \frac{fM_\oplus}{\bar{R}_\oplus c^2} = 6.969290134 \cdot 10^{-10}$;
- IAU2000 — The IAU2000 metric: $L_g = 0$;
- IERS1996 — The IERS1996 metric: $L_g = -\frac{fM_\oplus}{\bar{R}_\oplus c^2} = -6.969290134 \cdot 10^{-10}$;

3.6 Computation of path delay when one of the station is on orbit

Theory of computation of path delay when one of the station is on the orbit is given in section 2.1.2. The orbit ephemerise should be read with routine VTD_READ_NZO and then loaded with routine VTD_LOAD_NZO. The satellite ephemeris should conform to Orbit Data Messsages

CSSDS 502.0-B-2[2] standard issued by the Consultative Committee for Space Data Systems. Computation of path delay is done with the same routine as for computation of path delay between ground stations: VTD_DELAY. Effects of tides, antenna axis offsets, loadings, delay in the ionosphere and troposphere are not computed for the orbiting station. NB: VTD cannot compute path delay if the orbit is not available.

In the case of a satellite that does not have a sample counter, like Radioastron, clock synchronization is done implicitly at the moment of receiving the first sample of a scan. The light time between the orbiting station and the control downlink station (which is usually *different* than the ground observing station) should be computed and added to the path delay returned by VTD_DELAY. Routine VTD_LT_ORB makes this computation. The effective clock function of the orbiting station that should be used in data reduction is a sum of three terms: the clock function of the orbiting station that accounts for Hydrogen maser frequency variations, the clock station of the downlink station, and the light time between the orbiting and downlink station. The first (unknown) term affects all the samples. The second and third term affect only the first sample of a scan. The second term is computed from time comparison between the Hydrogen maser at the downlink station and the GPS clock and it is approximated by a polynomial of the first degree.

The term that describes time dilation (expression 19) is computed by routine VTD_REL_ORB. It has **two time arguments**: time synchronization epoch and observation epoch. NB: both time arguments should be given at a retarded moment of time, t_s. The difference $t_d - t_s$ is given by routine VTD_LT_ORB. This difference should be *subtracted* from time of observation. The result of VTD_REL_ORB, Δt, is *added* if the orbiting station is a reference station #1 or *subtracted* if the orbiting station is a remote station #2.

Reduction for clock for the ground station is made by computing a priori clock function from Hydrogen maser comparison and the GPS clock and applying this function to *every* sample. For reduction for time dilation with a continuous on-board sample counter, the first time epoch for routine VTD_REL_ORB is time of clock synchronization which usually takes place prior the observing session. For reduction for time dilation without a continuous on-board sample counter, the first epoch of VTD_REL_ORB is a time coordinate at the orbiting station at the moment *first sample of a given scan*, which is time of a downlink station minus light time $t_d - t_s$ given by routine VTD_LT_ORB.

The fundamental distinction of a case when an orbiting station without a continuous on-board sample counter from other cases that time delay and delay rate is a **function of two time arguments:** nominal scan start determined by a downlink clock and time of observation. If the orbiting station has a continuous on-board sample counter, then the first argument is time of clock synchronization at the beginning of the experiment. Its precise value with accuracy significantly better then the window of fringe search is irrelevant, since it will be solved for during parameter estimation anyway.

Thus, time delay for an orbiting station is a sum of three terms: delay returned by VTD_DELAY, light time returned by VTD_LT_ORB, and clock dilation returned by VTD_REL_ORB with an appropriate sign.

References

[Bowring, 1985] Bowring, B.R., 1985, The Accuracy of Geodetic Latitude and Height Equations", Survey Review, vol. 28, pp. 202–206.

[2] http://public.ccsds.org/publications/archive/502x0b2c1.pdf

[Capitaine et al.(2003a)] Capitaine, N., Chapront, J., Lambert, S., & Wallace, P. T., "Expressions for the Celestial Intermediate Pole and Celestial Ephemeris Origin consistent with the IAU 2000A precession-nutation model", *Astronomy and Astrophysics*, vol. 400, p. 1145, 2003

[Chen and Herring (1997)] Chen G., Herring T. A. "Effects of atmospheric azumithal assymetry on the analysis of space geodetic data", *Journal of Geophys. Res.*, 1997, vol. 102(B9), pp. 20,489–20,502.

[Davis (1985)] Davis, J.L., et al., "Geodesy by radio interferometry: Effects of atmospheric modeling errors on estimates of baseline length", Radio Science, 20, 1593-1607, 1985.

[Dehant et al., 1998] Dehant V., Defraigne P. and Wahr J. M, "Tides for a convective Earth", *Journal of Geophys. Res.*, 1998, vol. 104(B1), pp. 1035-1058.

[Dickman, 1993] Dickman, S.R, "Dynamic ocean-tide effects on Earth's rotation", *Geophys. J. Int.*, vol. 112, pp. 448-470, 1993.

[Goff & Gratch, 1946] Goff J.A., S. Gratch. Low-pressure properties of water from $-160°$ to $212°F$, *American society of heating and ventilating engeneers. Transactions*, **52**, pp. 95–129, 1946.

[Hartmann and Wenzel(1995)] Hartmann, T. and H.-G. Wenzel, The HW95 tidal potential catalogue, *Geophys. Res. Let.*, *22*, 3353–3356, 1995.

[Hrgian, 1975] Hrgian, A.H, ed., International meteorological tables, Ser. 1–2, Transactions of the Soviet meteorological association, vol. 94, Obninsk, 1975.

[Kopeikin and Shaeffer, 1999] Kopeikin, S. M. and Shaeffer G., Physical Review, D, vol. 50, 124002, 1999.

[Lieske et al., 1976] Lieske, J.H. and Lederle, T. and Fricke, W. & Morando, B., "Expressions for the precession quantaties based upon the IAU (1976) system of astronomical constants", *Astronomy & Astrophysics*, vol. 58, N1, pp. 1–17, 1977.

[*Mathews et al.*(1995)] Mathews, P.M., B.A. Buffett, and I.I. Shapiro, Love numbers for a rotating spheroidal Earth: New definitions and numerical values, *Geophys. Res. Let.*, *22*(5), 579–582, 1995.

[Mathews et al., 1997] Mathews P.M., Dehant V. and Gipson J. M. "Tidal Station Displacements", *Journal of Geophys. Res.*, 1997, vol. 102(B9), pp. 20469–20478

[*Mathews* (2001)] Mathews, P.M., Love numbers and gravimetric factor for diurnal tides, *Journal of the Geodetic Society of Japan*, *47*(1), 231–236, 2001.

[McMillan and Ma (1997)] McMaillan D.S. and Ma C. "Atmospheric gradients and the VLBI terrestrical and celestial reference frames", *Geophys. Res. Let.*, vol. 24, pp. 453–456, 1997.

[Matveenko et al.(1965)] Matveenko, L. I., Karadashev, A. C., Sholomitskij, G. B. 1965, Izvestia VUZov. Radiofizika, 8, 651 (in Russian).

[Niell (1996)] Niell, A.E., (1996). Global mapping functions for the atmosphere delay at radio wavelengths, *J. Geophys. Res.*, 101, No. B2, p. 3227–3246.

[Saastamoinen(1972a)] Saastamoinen J (1972a) Contributions to the theory of atmospheric refraction, Bull Geod, 105:279–298

[Saastamoinen(1972b)] Saastamoinen J (1972b) Introduction to practical computation of astronomical refraction. Part II Bull Geod, 106:383–397

[*Simon et al.*(1994)] Simon, J.L, P. Bretagnon, J. Chapront, M. Chapront-Touze, G., Francou, and J. Laskar, Numerical expressions for precession formulae and mean elements for the Moon and the planets, *Astronomy and Astrophysics*, *282*, 663–684, 1994.

[Sovers et al.(1998)] Sovers, O.J, J.L. Fanselow, and C.S. Jacobs, 1998, Review of Modern Physics, 70, 1393

[ISO (1975)] International Organization for Standardization, Standard Atmosphere, ISO 2533:1975, 1975 `http://en.wikipedia.org/wiki/International_Standard_Atmosphere`